MEANDER AND PEARLING OF SINGLE-CURVATURE BILAYER INTERFACES IN THE FUNCTIONALIZED CAHN-HILLIARD EQUATION

ARJEN DOELMAN,[*] GURGEN HAYRAPETYAN,[†] KEITH PROMISLOW,[‡] AND BRIAN WETTON[§]

Abstract. The functionalized Cahn-Hilliard (FCH) free energy models interfacial energy in amphiphilic phase separated mixtures. Its minimizers encompass a rich class of morphologies with detailed inner structure, including bilayers, pore networks, pearled pores and micelles. We address the existence and linear stability of α-single curvature bilayer structures in $d \geq 2$ space-dimensions for a family of gradient flows associated to the strong functionalization scaling. The existence problem requires the construction of homoclinic solutions in a perturbation of a 4th-order integrable Hamiltonian system while a negative index argument reduces the linear stability analysis to the characterization of the meander and pearling modes of the second variation of the FCH energy on a family of invariant subspaces, independent of the choice of mass-preserving gradient flow.

Key words. Functionalized Cahn-Hilliard, Meander, Pearling, Strong Functionalization

AMS subject classifications. 35B32, 35B35, 35G50, 35P15, 37L15, 92C15.

1. Introduction. A molecule or polymer is amphiphilic with respect to a solvent if it has components with both favorable and unfavorable energetic interactions with the solvent. Amphiphilic molecules are commonly used as surfactants, such as soap, but amphiphilic polymers are finding wide ranging applications to energy conversion materials due to their propensity to self assemble fine-scale, solvent-accessible interface and network morphologies, [24]. Amphiphilic polymers can be created through the "functionalization" of hydrophobic polymers via the addition of hydrophilic side-chains or end-groups, for example by atom transfer radical polymerization, [16]. The hydrophilic moieties seek to lower its free energy by residing inside the solvent phase, while the hydrophobic segments of the polymer phase separate from the solvent to the extent possible. When either the solvent or the functional component of the polymer are relatively scarce, the mixture can be approximated as two-phase, with a prescribed volume of the scarce phase residing exclusively on interfacial structures lined by the hydrophilic moiety. The interface thickness is typically established by molecular considerations and either forms bilayer structures (co-dimension one) which separate the dominant phase, or higher co-dimension structures, such as pore-networks, which may percolate through the dominant phase.

The hydrophobic element can form the minority phase when the polymer is relatively short. Lyotropic liquid crystals, such as lipids, are a classic example of this group of amphiphilic materials, with a short hydrophobic tail bonded to a hydrophilic end-group. When immersed in a bulk solvent phase the lipids assemble into a variety of thin structures, such as bilayers, pores, and micelles, [17]. In the bilayer regime the bulk solvent phase is partitioned by lipid bilayers whose hydrophilic head groups are exposed to the solvent while the hydrophobic tail groups are sequestered inside the bilayer. In the case of polymer electrolyte membranes (PEMs), it is the solvent phase that is scarce. PEMs are synthesized from hydrophobic polymers that have been functionalized via the addition of hydrophilic side-chains. The hydrophobic polymer forms a continuous, elastic matrix, but will imbibe solvent to hydrate the functional groups, up to a limit permit by the elastic deformation associated with the membrane swelling. The solvent phase typically arranges into a network morphology which wets the hydrophilic head groups within the polymer matrix, forming a charge-selective ion-conducting network. Based upon small-angle X-ray scattering (SAXS) data, it has been hypothesized, [11], that these conducting networks take a pearled-pore morphology.

The Functionalized Cahn-Hilliard (FCH) free energy has been proposed as a model for the interfacial energy associated with amphiphilic mixtures, [6, 7] and is similar to free energies derived from small-angle X-ray scatting data of amphiphilic mixtures, [8]. For a binary mixture with composition described by u on $\Omega \subset \mathbb{R}^3$, the FCH free energy takes the form

$$\mathcal{F}(u) = \int_\Omega \frac{1}{2} \left(\varepsilon^2 \Delta u - W'(u) \right)^2 - \varepsilon^p \left(\eta_1 \frac{\varepsilon^2}{2} |\nabla u|^2 + \eta_2 W(u) \right) \, dx, \tag{1.1}$$

where $\varepsilon \ll 1$ denotes the interfacial thickness. The function $W : \mathbb{R} \mapsto \mathbb{R}$ is a non-degenerate double-well potential with two, typically *unequal* depth wells which we take at $u = -1$ and $u = m > 0$. Moreover we assume $W'(u)$

---
[*]Mathematisch Instituut, Universiteit Leiden, the Netherlands, doelman@math.leidenuniv.nl.
[†]Department of Mathematical Sciences, Carnegie Mellon University, U.S.A., ghayrap@andrew.cmu.edu.
[‡]Department of Mathematics, Michigan State University, U.S.A., kpromisl@math.msu.edu.
[§]Mathematics Department, University of British Columbia, Canada, wetton@math.ubc.ca.

has 3 zeroes, at $u = -1, 0, m$, that are strict local extrema, with $\mu_- := W''(-1) > 0$ and $\mu_+ := W''(m) > 0$, while $\mu_0 := W''(0) < 0$. The functionalization terms, multiplied by the functionalization parameters, η_1 and η_2, are made small by the factor of ε^p, p typically 1 or 2, in comparison to the dominant term arising from the square of the gradient term. Indeed, subject to zero-net flux boundary conditions, such as period or appropriate extensions of Neumann conditions, see [20], minimizers of the FCH energy must render the squared-gradient term small. Consequently, such functions u are proximal to the critical points of the associated Cahn-Hilliard free energy,

$$\mathcal{E}(u) := \int_\Omega \frac{\varepsilon^2}{2} |\nabla u|^2 + W(u) \, dx, \tag{1.2}$$

that is, solutions of

$$\frac{\delta \mathcal{E}}{\delta u}(u) := -\varepsilon^2 \Delta u + W'(u) = 0. \tag{1.3}$$

For $\eta_1 > 0$ the corresponding minimizers of the functionalized Cahn-Hilliard are selected from the *saddle points* of the associated Cahn-Hilliard type free energy, with the particular saddle points chosen depending sensitively upon the values of the functionalization parameters.

There are two natural distinguished limits of the FCH energy. The strong functionalization, for which $p = 1$, is the case we study in this work. It leads to a morphological competition mediated by total curvature and a bifurcation structure which depends primarily upon the functionalization parameters and the shape of the potential well $W(u)$, [14]. The weak functionalization corresponds to $p = 2$, as is consistent with the Γ-limit scaling for higher-order variants of the Cahn-Hilliard energy, see [21], and leads to competitive morphological evolution on a slower time-scale through Willmore type flows involving cubic terms in the curvature and surface diffusion that support bistability of network morphologies of distinct co-dimension, [4]. In either scaling, $\eta_1 > 0$, characterizes the strength of the hydrophilicity of the amphiphilic phase, while $\eta_2 \in \mathbb{R}$, models pressure differences between the majority and minority phases. The pressure differences arise from a variety of effects, including osmotic pressure of the counter ions within the solvent phase of the PEM membranes, [19, 15], or in the case of lipids, from crowding of tail groups within the hydrophobic domain, [7].

The slow relaxation of chemical systems is typically over-damped and thus is well modeled by the gradient flow of a free energy. The choice of the gradient is often hard to motivate from practical considerations, and correspondingly we consider a broad class of *admissible gradients* $\mathcal{G}$, that are non-negative, self-adjoint operators on the Sobolev space $H_N^s(\Omega)$ associated to appropriate zero-net flux boundary conditions for some $s \geq 1$. In particular we assume that the kernel of $\mathcal{G}$ is spanned by the constant functions, and that $\mathcal{G}$ is uniformly coercive in $L^2(\Omega)$ over $\ker(\mathcal{G})^\perp \cap H_N^s(\Omega)$ with a self-adjoint square root $\mathcal{G}^{\frac{1}{2}}$. The kernel of $\mathcal{G}$ guarantees that the gradient flow of the FCH free energy

$$u_t = -\mathcal{G} \left((\varepsilon^2 \Delta - W''(u) + \varepsilon^p \eta_1)(\varepsilon^2 \Delta u - W'(u)) + \varepsilon^p \eta_d W'(u) \right) = -\mathcal{G} \frac{\delta \mathcal{F}}{\delta u}, \tag{1.4}$$

is mass-preserving when subject to zero-flux boundary conditions. Here we have introduced $\eta_d := \eta_1 - \eta_2$. Typical choices for $\mathcal{G}$ are $\mathcal{G} = -\Delta$ [3, 4], which corresponds to the H^{-1} gradient flow of the FCH energy and the zero-mass projection over Ω,

$$\mathcal{G} = \Pi_0 f := f - \frac{1}{|\Omega|} \int_\Omega f(x) \, dx \tag{1.5}$$

[6, 9], which is also the orthogonal projection onto $\ker(\mathcal{G})$. The non-local, regularized Laplacian gradient $\mathcal{G} = -\Delta/(1 - \ell \Delta)$, for $\ell > 0$ is also of interest as are other convolution terms. The evolution (1.4) is a gradient flow in the sense that

$$\frac{d}{dt} \mathcal{F}(u(t)) = - \left\| \mathcal{G}^{\frac{1}{2}} \frac{\delta \mathcal{F}}{\delta u} \right\|_{L_\Omega^2}^2 \leq 0. \tag{1.6}$$

In this work, we consider the strong functionalization scaling $p = 1$ in (1.1), (1.4). We establish the existence of (stationary) bilayer equilibria corresponding to co-dimension one interfaces with a fixed number of identical, constant, non-zero curvatures and a complimentary number of zero curvatures. We characterize in full analytical

detail the spectra associated to the linear stability of these $\alpha-$single curvature bilayers. In prior work, [6, 3, 4], the evolution of general interfacial structures of bilayers (or pores) has been determined by a multiple-scale approach, under the *assumption* that the evolving structures are linearly stable. The present work complements these studies in the sense that the stationary α-single curvature structures correspond to the most simple critical points of the FCH gradient flows. However, by the formal nature of the derivation process, the evolution equations obtained in [6, 3, 4] represent leading-order approximations that are only valid on limited timescales. The critical points we construct are exact solutions of governing equations (1.1), (1.4). Although our approach is also asymptotic, both the existence and the linear stability of the single-curvature bilayers are rigorous – the existence problem is settled by establishing that certain stable and unstable manifolds intersect transversely. Thus, the present work provides a rigorous foundation for some aspects of these prior results. The general structure of the linearized operators associated to bilayer interfaces was addressed in [9], in particular the coercivity of the operators on spaces orthogonal to the pearling and meander eigenvalues was established. However the bifurcation structure of these modes has not been analytically characterized: the linear stability of the evolving bilayer (or pore) structures has been assumed. In experimental settings, the pearling instability occurs naturally in bilayer structures, it signals their transformation to gyroid and pore network morphologies, see [17]. In this paper, we obtain full analytic control over spectrum associated to (possible) pearling.

To highlight the generality of our approach we not only work with a general admissible gradient $\mathcal{G}$ but we also consider a bounded domain $\Omega \subset \mathbb{R}^d$ for arbitrary $d \geq 2$. However, we restrict the geometry of the co-dimension one bilayer interface, Γ immersed in Ω, to the simplest class which permits an investigation of the full impact of curvature and space dimension upon the linear stability. Specifically we consider co-dimension one, α-single curvature interfaces, Γ, which possess constant curvature $k = -1/R_0$ in $\alpha \in [0, d-1] \cap \mathbb{Z}$ directions and zero curvature in the remaining $K := d - \alpha - 1 \geq 0$ directions. These are higher dimensional generalizations of cylinders and spheres: in $\mathbb{R}^3$ they include the spherical ($\alpha = 2$), cylindrical ($\alpha = 1$), and flat ($\alpha = 0$) interfaces. For simplicity of presentation we fix the domain with the same symmetry as the interface,

$$\Omega = R_b \overline{S}_\alpha \times \prod_{j=1}^{K} [0, L_j], \tag{1.7}$$

where $\overline{S}_\alpha$ is the solid unit sphere in $\mathbb{R}^{\alpha+1}$, $R_b > R_0$, and $L_j > 0$ for $j = 1, \ldots, K$, see Figure 2.1. The cylindrical interfaces, for which $K > 0$, intersect $\partial\Omega$, while the purely spherical surfaces, with $K = 0$, are disjoint from $\partial\Omega$. The advantage of this choice of Ω is that for an α-single curvature interface Γ whose axis of symmetry aligns with that of Ω, the signed distance function, $\rho(x)$, of $x \in \Omega$ to Γ is well-defined in all of Ω.

For α-single curvature interfaces, the existence problem associated to (1.4) reduces to an ODE in the radial coordinate R – this is the spherical radius in the $\alpha = 2$ case in $\mathbb{R}^3$ or the cylindrical radius of the cylinder for the $\alpha = 1$ cylinder in $\mathbb{R}^3$. The free parameter R_0 sets the radius of the spherical dimensions of the α-single curvature interface Γ, or equivalently through $k = -1/R_0$, the (constant) local curvature of the interface Γ. However the problem is more naturally and generally studied in the curvilinear coordinates via the signed, ε-scaled distance r to Γ, defined as $R = R_0 + \varepsilon r$, see section 2. We establish the existence of a homoclinic solution $u_h(r)$ to the fourth-order problem,

$$\left(\frac{d^2}{dr^2} + \frac{\varepsilon\alpha}{R_0 + \varepsilon r} \frac{d}{dr} - W''(u) + \varepsilon\eta_1 \right) \left(u_{rr} + \frac{\varepsilon\alpha}{R_0 + \varepsilon r} u_r - W'(u) \right) + \varepsilon\eta_d W'(u) = \varepsilon\gamma, \tag{1.8}$$

where $\varepsilon\gamma$ is a free constant that spans the kernel of $\mathcal{G}$, see section 3 for the details. The main existence result for non-flat interfaces ($\alpha > 0$) is formulated as follows.

THEOREM 1.1. **(Existence)** *Fix $\alpha > 0, R_0 > 0$, and $\eta_1, \eta_2 = \mathcal{O}(1) \in \mathbb{R}$ and assume that $W(u)$ is a non-degenerate double well potential, and that ε is small enough. Then there exists a unique function $\gamma_h(\varepsilon) = O(1)$ such that for the choice $\gamma = \gamma_h$ the solvability condition (3.13) holds and there is a unique $u_- := -1 + \mathcal{O}(\varepsilon)$ such that existence problem (1.8) has a homoclinic solution $u_h = u_h(r; \alpha, R_0)$ that approaches the rest state u_- of (1.8) as $|r| \to \infty$.*

This result is established by writing (1.8) as a 4-dimensional dynamical system. The proof relies crucially on the observation that (1.8) has an explicitly constructible Hamiltonian in the (flat) limit $R_0 \to \infty$ and that the system is completely integrable in the limit $\varepsilon \downarrow 0$ – see section 3 and especially Theorem 3.1 and its proof. The flat $R_0 \to \infty$ case is special, in the sense that the homoclinic solution $u_h(r)$ exists for all γ – i.e. there is no solvability condition to satisfy – see Corollary 3.2. In Corollary 3.3, the results of Theorem 1.1/3.1 are modified to fit into the bounded domain Ω (1.7). The α-single curvature bilayer morphologies

$U_{h,b}(x) := u_{h,b}(r(x)) \in H^4(\Omega)$ that satisfy homogeneous Neumann boundary conditions are obtained from Γ by dressing it with the solution $u_{h,b}$ that is exponentially close to the homoclinic solution $u_h := u_h(r; \alpha, R_0)$; details of the 'dressing' procedure are presented in section 2.

The main body of work, addressed in section 4, concerns the linear stability analysis of the α-single curvature bilayers $U_{h,b}(x) \in H^4(\Omega)$. The analysis is a novel combination of classical – but quite subtle – asymptotic analysis with functional analytic insights on the structure of the associated spectral operator based on the geometrical nature of the problem. Our main result is an analysis of the *negative space* associated to the self-adjoint operator $\mathbb{L}$, defined in (4.2), given by the second variational derivative of $\mathcal{F}$ at $U_{h,b}$ and its sharp correlation to the number of positive eigenvalues of $-\mathcal{G}\mathbb{L}$, the linearization of (1.4) about $U_{h,b}(x)$. The negative space of $\mathbb{L}$ is the largest linear space on which the bilinear form $\langle \mathbb{L}u, u \rangle_\Omega$ is non-positive, in particular its dimension equals that of the negative eigenspaces of $\mathbb{L}$, and by Lemma 4.1 detects instabilities associated to $-\mathcal{G}\mathbb{L}$. In particular, we use the negative index to develop rigorous asymptotics for the mass-conservation eigenvalue, this step is heart of the reduction of the linear stability of α-single curvature bilayers $U_{h,b}(x)$ to the asymptotic analysis of $\mathbb{L}$, see section 4

This analysis identifies two types of potential instabilities: those associated to $\mathcal{O}(1)$ wave-length deformations of the interface, called *meander* instabilities, and those associated to $\mathcal{O}(\varepsilon^{-1})$ wave length modulations of the interfacial thickness, termed *pearling* instabilities, see Figure 4.2. More precisely, our analysis establishes that these are the only two mechanisms that may destabilize an α-single curvature bilayer. Our central theorem is the following sharp classification of the onset of these instabilities for non-flat ($\alpha \neq 0$) interfaces.

THEOREM 1.2. **(Linear stability)** *Consider the strong FCH gradient flow, (1.4), with $p = 1$, an admissible gradient $\mathcal{G}$, and a non-degenerate double-well potential $W(u)$, subject to zero-flux boundary conditions on $\Omega \subset \mathbb{R}^d$ (1.7) in space dimension $d \geq 2$. Suppose that $\alpha = 1, 2$, or $d - 1$ – which exhausts all cases if $d \leq 4$ – and that ε is small enough. Then, the α-single curvature bilayer equilibrium $U_{h,b} \in H^4(\Omega)$ constructed in Corollary 3.3 is linearly stable with respect to the FCH gradient flow if and only if the pearling condition (4.32) holds. Moreover there exists a constant $C_1 > 0$, independent of ε, such that $\sigma(-\mathcal{G}\mathbb{L}) \backslash \{0\} \subset (-\infty, -C_1\varepsilon^4]$ with the kernel of $-\mathcal{G}\mathbb{L}$ spanned by the translational symmetries and the mass-constraint eigenvalue $\mathbb{L}^{-1}1$.*

If $d \geq 5$ and $\alpha = 3, \cdots, d - 2$, stability to meander perturbations in the flat direction of Γ requires the additional geometric constraint that (4.65) does not hold for μ_1 as defined in (4.12).

Hence, up to dimension $d = 4$, all possible α-single curvature bilayers are (linearly) stable with respect to the meander destabilization mechanism, and so are all spherical bilayers ($\alpha = d - 1$ in $\mathbb{R}^d$). Only in dimension $d \geq 5$, cylindrical α-single curvature bilayers with $3 \leq \alpha \leq d - 2$ may be destabilized by the meander instability. In all cases, the stability with respect to the pearling instability is determined by condition (4.32) – a condition that gives very explicit information on the impact of the main parameters η_1 and η_2, as well as the shape of the double-well potential $W(u)$, on the possible occurrence of the pearling destabilization.

The proof of Theorem 1.2 is separated into partial results established in section 4. We refer to section 4.2 for on overview of how Theorem 1.2 follows from these partial results. A corresponding analysis of the stability of flat interfaces, $\alpha = 0$, is given in section 4.6. In the context presented here, the flat case should not be viewed as an infinite radius limit, $R_0 \to \infty$, of a curved interface. Indeed, a continuous deformation of a curved bilayer into a flat interface requires an infinite domain, Ω, and our results, particularly Lemma 4.8, require that the volume, $|\Omega|$, be $\mathcal{O}(1)$. Through our analysis, we find that the flat case is special. Both the pearling and the meander mechanisms may destabilize a flat bilayer, consequently a stable flat bilayer requires two conditions, a pearling condition (4.72) that is in essence identical to that of Theorem 1.2, and an explicit meander condition (4.73) – see Corollary 4.9.

Finally in section 5 we refine the stability analysis for a particular class of potential wells for which explicit evaluations of the stability conditions are possible. This yields detailed insight on the impact of the shape of the potential well $W(u)$ on the stability of the α-single curvature bilayers. This is particularly relevant to the flat case since it clearifies, that the two conditions stability conditions (4.72) and (4.73) and not mutually exclusive. We conclude the paper by comparing the outcome of our analysis to numerical simulations.

2. Curvilinear coordinates and notation. Smooth, co-dimension one interfaces, Γ, which are far from self-intersection admit a local coordinate system involving the signed, ε-scaled distance r to the interface, and tangential variables $s = (s_1, \ldots, s_{d-1})$. The associated change of variables takes the form

$$x = \rho(s, r) := \zeta(s) + \varepsilon r n(s), \qquad (2.1)$$

where $\zeta : \hat{\Gamma} \subset \mathbb{R}^{d-1} \mapsto \Gamma \subset \mathbb{R}^d$ is a local parameterization of Γ and n is the normal to Γ. The inverse map is denoted $s = s(x)$ and $r = r(x)$ for x sufficiently close to Γ. In this curvilinear coordinate system the cartesian
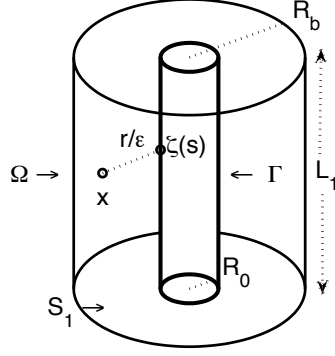
FIG. 2.1. *Depiction of the a 1-single curvature interface* Γ, *a cylinder, immersed in* $\Omega \subset \mathbb{R}^3$, *showing the notation of (1.7), and the associated scaled distance function* $r = r(x)$.

Laplacian transforms to

$$\Delta = \varepsilon^{-2}\partial_r^2 + \varepsilon^{-1}\kappa(s,r)\partial_r + \Delta_G, \tag{2.2}$$

where we have introduced the extended curvature

$$\kappa(s,r) := \frac{\partial_r J}{\varepsilon J} = -\sum_{i=1}^{d-1} \frac{k_i(s)}{1 - \varepsilon r k_i(s)}, \tag{2.3}$$

the Jacobian, $J = J(s,r)$, of the parameterization $x = \rho(s,r)$ of Γ, and the curvatures $\{k_i\}_{i=1}^{d-1}$ of Γ. The operator Δ_G is defined in terms of the $(d-1) \times (d-1)$ metric tensor, $\mathbf{G}$, of Γ by

$$\Delta_G := J^{-1} \sum_{i,j=1}^{d-1} \frac{\partial}{\partial s_i} \left(G^{ij} J \frac{\partial}{\partial s_j} \right), \tag{2.4}$$

where G^{ij} denotes the ij element of $\mathbf{G}^{-1}$. Moreover the operator admits the formal expansion

$$\Delta_G = \Delta_s + \varepsilon r \Delta_s^{(1)} + \varepsilon^2 r^2 \Delta_s^{(2)} + O(\varepsilon^3 r^3), \tag{2.5}$$

where Δ_s is the Laplace-Betrami operator associated to Γ and $\Delta_s^{(j)}$ for $j = 1, 2, \dots$ are second-order differential operators in s, see [9, 3] for details.

Our equilibrium morphologies are based on α-single curvature interfaces Γ embedded in $\Omega \subset \mathbb{R}^d$. For simplicity of presentation, we assume that $\Omega \subset \mathbb{R}^d$ possesses the same symmetry as the surface Γ, taking the form (1.7), and orient it and the cartesian coordinate system along a major axis of the symmetry. In the local coordinates foliate al of Ω, which takes the form of a generalized cylinder $\hat{\Gamma} \times [-R_0/\varepsilon, R_b/\varepsilon]$, and the $L^2(\Omega)$ inner product takes the local variable form,

$$\langle f, g \rangle_{L^2(\Omega)} = \int_{\hat{\Gamma}} \int_{-R_0/\varepsilon}^{R_b/\varepsilon} f(r,s) g(r,s) J(r,s) \, dr \, ds. \tag{2.6}$$

With these assumptions, both the size of Ω and the distance of Γ to $\partial\Omega$ are $O(1)$ in the unscaled variables.

For an α-single curvature interface the curvilinear coordinates $s = (s_1, \dots, s_{d-1})$ can be decomposed into $s = (\theta, \tau)$ where $\theta = (\theta_1, \dots, \theta_\alpha)$, parameterize the directions with curvature $k = -R_0^{-1}$, and $\tau = (\tau_1, \dots, \tau_K)$, for $K = d - \alpha - 1$, parameterize the flat directions of the interface. As a result, the Laplacian expression simplifies to

$$\varepsilon^2 \Delta = \partial_r^2 + \varepsilon \kappa(r) \partial_r + \varepsilon^2 \left(\Delta_\tau + \frac{1}{(R_0 + \varepsilon r)^2} \Delta_\theta \right), \tag{2.7}$$

where Δ_τ is the usual Laplacian in τ, and Δ_θ is the Laplace-Beltrami operator for the unit sphere in $\mathbb{R}^{\alpha+1}$, and the extended curvature takes the form

$$\kappa(r) = \frac{\alpha}{R_0 + \varepsilon r}. \tag{2.8}$$

Moreover the Jacobian takes the simple form

$$J(r) = \varepsilon J_\alpha(\theta) (R_0 + \varepsilon r)^\alpha, \tag{2.9}$$

where J_α is the Jacobian associated to the unit sphere in $\mathbb{R}^{\alpha+1}$.

Given an α-single curvature interface Γ and $\phi \in L^2(\mathbb{R})$ which decays exponentially, with an $O(1)$ rate to $\phi_\infty \in \mathbb{R}$ as $r \to \pm\infty$, we define the ϕ-dressing of Γ as the function $\phi \in L^2(\Omega)$, defined by $\phi(x) = \phi(r(x))$. Up to exponentially small terms we may write the integral of a ϕ-dressing of Γ as

$$\begin{aligned} \int_\Omega (\phi(x) - \phi_\infty)\,dx &= \int_{\hat{\Gamma}} \int_{\mathbb{R}} (\phi(r) - \phi_\infty)\varepsilon J_\alpha(\theta)(R_0 + \varepsilon r)^\alpha\, dt\, d\theta\, dr, \\ &= \varepsilon|\Gamma| \int_{\mathbb{R}} (\phi(r) - \phi_\infty)(R_0 + \varepsilon r)^\alpha\, dr. \end{aligned} \tag{2.10}$$

The $L^2(\Omega)$ norm of $U \in L^2(\Omega)$ is denoted $\|U\|_{L^2_\Omega}$ with inner produce $\langle \cdot, \cdot \rangle_\Omega$. However if $U = U(x) = u(r(x))$ is the u dressing of Γ by $u \in L^p(\mathbb{R})$, then we will also have recourse to the $L^p(\mathbb{R})$ norm of u, which we denote $\|u\|_p$ with the inner product corresponding to $p = 2$ denoted by $\langle \cdot, \cdot \rangle_2$.

3. The existence of α-single curvature bilayer equilibria. In this section we show that for a fixed α-single curvature interface Γ, the dressing technique introduced in Section 2 permits the construction of a stationary solution of the full problem (1.4) from a homoclinic solution of an associated fourth-order ODE in the signed distance variable r. The dressing of Γ with a homoclinic solutions yields a function which is constant in the tangential variables, s, and exponentially small on $\partial\Omega$, and can be modified to be an exact solution using standard techniques.

Bilayer structures are formed by "dressing" a co-dimension one manifold $\Gamma \subset \mathbb{R}^d$, $d \geq 2$, with a critical point of the FCH energy which is homoclinic to a spatially constant background state. Since the kernel of $\mathcal{G}$ is spanned by the constants, stationary solutions of (1.4) satisfy

$$\left(\varepsilon^2\Delta - W''(u) + \varepsilon\eta_1\right)\left(\varepsilon^2\Delta u - W'(u)\right) + \varepsilon\eta_d W'(u) = \varepsilon\gamma, \tag{3.1}$$

subject to appropriate boundary conditions, with γ taking the form

$$\gamma = \gamma_1 + \varepsilon\gamma_2 + \mathcal{O}(\varepsilon^2). \tag{3.2}$$

For a particular choice of α we look for solutions of $U_h(x; \alpha) = u_h(r; \alpha)$ of (3.1) which are independent of the in-plane variables s. With this assumption (2.7) reduces to

$$\varepsilon^2\Delta = \partial_r^2 + \frac{\varepsilon\alpha}{R_0 + \varepsilon r}\partial_r = \partial_r^2 + \frac{\varepsilon\alpha}{R_0}\left[1 - \frac{r}{R_0}\varepsilon + \frac{r^2}{R_0^2}\varepsilon^2 + \mathcal{O}(\varepsilon^3)\right]\partial_r, \tag{3.3}$$

and introducing $v = v(r)$ through the relation $u_{rr} - W'(u) = \varepsilon v$ it is possible, with some algebraic reorganization, to rewrite the system (3.1) as two, coupled second-order equations

$$\begin{cases} \ddot{u} - W'(u) &= \varepsilon v, \\ \ddot{v} - W''(u)v &= [\gamma_1 - \eta_d W'(u)] + \varepsilon\left[\gamma_2 - \frac{2\alpha}{R_0}\dot{v} + \frac{\alpha(2-\alpha)}{R_0^2}W'(u) - \eta_1 v - \frac{\alpha}{R_0}\eta_1\dot{u}\right] + \mathcal{O}(\varepsilon^2), \end{cases} \tag{3.4}$$

where the dot denotes ∂_r. This can also be viewed as a fourth-order system in $(u, p = \dot{u}, v, q = \dot{v})$.

3.1. Basic properties of the existence ODE. The system (3.4) has 3 critical points, but we assume that the $u = -1$ phase is dominant and consider orbits homoclinic to the equilibrium $P_- = (\bar{u}_-, \bar{p}_-, \bar{v}_-, \bar{q}_-) = (\bar{u}_-, 0, \bar{v}_-, 0)$ where $\bar{u}$ and $\bar{v}$ satisfy

$$(\bar{u}_-, \bar{v}_-) = \left(-1, -\frac{\gamma_1}{\mu_-}\right) + \mathcal{O}(\varepsilon), \tag{3.5}$$

where $\mu_- = W''(-1)$. The linearization of the fourth-order version of (3.4) about P_- yields a 4×4 matrix with the spectrum,

$$\lambda_{\pm,\pm} = \pm\sqrt{\mu_-} \pm \frac{1}{2\mu_-}\sqrt{\varepsilon}\sqrt{-\gamma_1 W'''(-1) - \eta_d\mu_-^2} + \mathcal{O}(\varepsilon).$$

Since $\mu_- > 0$, we infer that the stable and unstable manifolds $W^s(P_-)$ and $W^u(P_-)$ of P_- are both 2-dimensional.

The system (3.4) is $\mathcal{O}(\varepsilon)$-close to two integrable limits. For any $\varepsilon \geq 0$ the 'flat limit', obtained by either letting $R_0 \to \infty$ or setting $\alpha = 0$ in (3.4), yields the flat system,

$$\left(\partial_r^2 - W''(u) + \varepsilon\eta_1\right)\left(\ddot{u} - W'(u)\right) + \varepsilon\eta_d W'(u) = \varepsilon\gamma, \tag{3.6}$$

which is an integrable Hamiltonian system with integral

$$H = \eta_1\left[\frac{1}{2}p^2 - W(u)\right] + pq - vW'(u) - \gamma u + \eta_d W(u) - \frac{1}{2}\varepsilon v^2, \tag{3.7}$$

that can be derived by multiplying (3.6) by $\dot{u}$, integrating over r, and using several identities. Moreover, for any $R_0 \geq 0$, the $\varepsilon \to 0$ limit of (3.4) is also fully integrable. Indeed substituting $\varepsilon = 0$ into (3.4) uncouples the u and v equations, leaving a planar system for u,

$$\ddot{u} - W'(u) = 0, \tag{3.8}$$

and a v-equation that coincides with an inhomogeneous version of the linearized u-equation. The $\varepsilon = 0$ system has two integrals,

$$K_1 = \frac{1}{2}p^2 - W(u), \quad K_2 = pq - vW'(u) - \gamma_1 u + \eta_d W(u), \tag{3.9}$$

where K_2 can be obtained from the $\ddot{v}$-equation by using its similarity to the linearization of the $\ddot{u}$-equation (i.e. set $v = \tilde{v}\dot{u}$ and integrate the resulting equation for $\ddot{\tilde{v}}$). Using the expansion (3.2) we observe that

$$H = \eta_1 K_1 + K_2 - \varepsilon(\frac{1}{2}v^2 - \gamma_2 p) + \mathcal{O}(\varepsilon^2).$$

Moreover for $\varepsilon \neq 0$ we have the slow evolution

$$\begin{aligned}
\dot{K}_1 &= \varepsilon\left[pv\right], \\
\dot{K}_2 &= \varepsilon\left[vq + p\left(\gamma_2 + \frac{\alpha(2-\alpha)}{R_0^2}W'(u) - \eta_1 v - \frac{\alpha}{R_0}(2q + \eta_1 p) + \mathcal{O}(\varepsilon)\right)\right], \\
\dot{H} &= \varepsilon\left[\frac{\alpha}{R_0}p\left(\frac{2-\alpha}{R_0}W'(u) - (2q + \eta_1 p) + \mathcal{O}(\varepsilon)\right)\right].
\end{aligned} \tag{3.10}$$

3.2. The main existence results. The homoclinic solution u_0 of the uncoupled system (3.8) plays a fundamental role in the construction of the homoclinic orbits of the $\varepsilon \neq 0$ system. Note that since u_0 is a homoclinic solution of a second order system with reflective symmetry ($r \mapsto -r$), we may take u_0 to be even about $r = 0$ after translation. Further, we introduce the linearization,

$$\mathcal{L} := \partial_r^2 - W''(u_0(r)), \tag{3.11}$$

of (3.8) about u_0. From standard Sturm-Liouville theory $\mathcal{L}$ has a simple kernel on $L^2(\mathbb{R})$, spanned by $\dot{u}_0$. Consequently we may define $v_0(r) = v_0(r;\gamma_1) \in L^\infty(\mathbb{R})$, the unique, bounded, even solution of the inhomogeneous problem,

$$\mathcal{L}v_0 = \gamma_1 - \eta_d W'(u_0). \tag{3.12}$$

Note that the right hand side of (3.12) is even, and that $\dot{u}_0$ odd, so that $\int_{\mathbb{R}}(\gamma_1 - \eta_d W'(u_0))\dot{u}_0\,dr = 0$. Hence, (3.12) is solvable, with a one-parameter family of solutions, spanned by the unique bounded *even* solution v_0 + the kernel of $\mathcal{L}$. Our first result is the existence of a homoclinic solution to the saddle point P_- in (3.4).

THEOREM 3.1. **(Existence)** *Fix* $\eta_d, \eta_1 = \mathcal{O}(1) \in \mathbb{R}$, $R_0 > 0$, *and the morphological index* $0 < \alpha \leq d - 1$. *We assume that W is a non-degenerate double well potential, and ε is small enough. Then there exists a unique* $\gamma_h = \gamma_h(\varepsilon) = \gamma_1 + \mathcal{O}(\varepsilon)$ *that solves*

$$\int_{\mathbb{R}} \left[2\dot{u}_0(r)\dot{v}_0(r;\gamma_1) + \eta_1 \dot{u}_0^2(r) \right] dr = 0. \tag{3.13}$$

such that the stable and unstable manifolds of P_- under (3.4), $W^s(P_-)$ and $W^u(P_-)$ respectively, intersect transversally yielding an orbit $\Gamma_h(r) = (u_h(r), p_h(r), v_h(r), q_h(r))$ homoclinic to P_-. Moreover Γ_h is close to $\Gamma_0 := (u_0(r), \dot{u}_0(r), v_0(r), \dot{v}_0(r))$, *in the sense that $\|\Gamma_h - \Gamma_0\|_\infty = \mathcal{O}(\varepsilon)$.*

Note that since $\Gamma_h(r)$ is homoclinic to P_- – given by (3.5) – Theorem 1.1 indeed immediately follows from Theorem 3.1.

The expression (3.13) for the existence of the homoclinic Γ_h can be further simplified. Observing that

$$\mathcal{L}(r\dot{u}_0) = 2\ddot{u}_0, \tag{3.14}$$

the first term in the existence integral simplifies via integration by parts and the self-adjointness of $\mathcal{L}$,

$$2 \int_{\mathbb{R}} \dot{v}_0 \dot{u}_0 \, dr = -2 \int_{\mathbb{R}} v_0 \ddot{u}_0 \, dr = -2 \int_{\mathbb{R}} v_0 \mathcal{L} \left(\frac{1}{2} r \dot{u}_0 \right) dr = -\int_{\mathbb{R}} (\mathcal{L} v_0) (r \dot{u}_0) \, dr. \tag{3.15}$$

Using the relation (3.12), integrating by parts, and finally integrating (3.8) we obtain,

$$2 \int_{\mathbb{R}} \dot{v}_0 \dot{u}_0 \, dr = -\int_{\mathbb{R}} (\gamma_1 - \eta_d W'(u_0)) (r\dot{u}_0) \, dr = \gamma_1 M_0 - \frac{1}{2} \eta_d \|\dot{u}_0\|_2^2, \tag{3.16}$$

where we have introduced the mass per unit length

$$M_0 := \int_{\mathbb{R}} (u_0 + 1) \, dr, \tag{3.17}$$

associated to the leading order bilayer profile, u_0. The existence condition (3.13) can be explicitly solved for γ_1,

$$\gamma_1 = \frac{\|\dot{u}_0\|_2^2}{2M_0} (\eta_d - 2\eta_1) = -\frac{\|\dot{u}_0\|_2^2}{2M_0} (\eta_1 + \eta_2). \tag{3.18}$$

Indeed, this choice of γ_1 fixes the $O(\varepsilon)$ coefficient of the far-field limit for equilbria u_h associated to non-zero curvature, see (3.23) and (3.27). The 'existence condition' (3.13) appears in the analysis with a pre-factor $\frac{\alpha}{R_0}$, see (3.21), and disappears in the flat, Hamiltonian limit $R_0 \to \infty$, for which $\alpha = 0$. This leads to the following result.

COROLLARY 3.2. *Fix $\eta_d, \eta_1 = \mathcal{O}(1) \in \mathbb{R}$ and let W be a non-degenerate double-well potential. In the flat case, $\alpha = 0$, the manifolds $W^s(P_-)$ and $W^u(P_-)$ of the system (3.6) intersect transversally for any given* $\gamma = \mathcal{O}(1) \in \mathbb{R}$, *see (3.2). The associated homoclinic orbit Γ_h is reversible and satisfies $\|\Gamma_h - \Gamma_0\|_{L^\infty} = \mathcal{O}(\varepsilon)$.* Corollary 3.2 is an intuitive result, in the flat ($\alpha = 0$) case the 2-dimensional manifolds $W^s(P_-)$ and $W^u(P_-)$ are both embedded in the 3-dimensional level set $H(u, p, v, q) = H(P_-)$: one generically expects a 1-dimensional intersection.

Proofs of Theorem 3.1 and Corollary 3.2. The leading order approximations of $W^s(P_-)$ and $W^u(P_-)$ can be determined directly from (3.4),

$$W^{u,s}(P_-) = \left\{ \Gamma_0(r - r_0) + D_0^{u,s}(0, 0, \dot{u}_0(r - r_0), \ddot{u}_0(r - r_0)) \,\middle|\, r_0, D_0^{u,s} \in \mathbb{R} \right\} + \mathcal{O}(\varepsilon), \tag{3.19}$$

where the free constants $D_0^{u,s}$ and r_0 parameterize the two-dimensional manifolds for $r \in (-\infty, r_0 + \mathcal{O}(1))$ for $W^u(P_-)$ and $r \in (r_0 - \mathcal{O}(1), \infty)$ for $W^s(P_-)$. Using (3.19), we can determine the total, accumulated, changes $\Delta^{u,s} K_{1,2}$ and $\Delta^{u,s} H$ in the perturbed integrals $K_{1,2}$ and H for orbits in $W^{u,s}(P_-)$ that travel from P_- to the hyperplane $\{p = 0\}$ or vice versa. All orbits in $W^{u,s}(P_-)$ intersect $\{p = 0\}$ and hence we can take the initial conditions (in forward or backward time) in the section $\{p = 0\}$ by setting $r_0 = 0$ in (3.19). Starting with K_1 we define

$$\Delta^u K_1 := \int_{-\infty}^0 \dot{K}_1 dr, \quad \Delta^s K_1 := -\int_0^\infty \dot{K}_1 dr,$$

so that, by (3.10) and (3.19),

$$\begin{array}{rcl}
\Delta^u K_1 &=& \varepsilon\left[\int_{-\infty}^0 \dot{u}_0 v_0 dr + D_0^u \int_{-\infty}^0 \dot{u}_0^2 dr\right] + \mathcal{O}(\varepsilon^2), \\
\Delta^s K_1 &=& -\varepsilon\left[\int_0^\infty \dot{u}_0 v_0 dr + D_0^s \int_0^\infty \dot{u}_0^2 dr\right] + \mathcal{O}(\varepsilon^2).
\end{array}$$

The Melnikov condition, $\Delta^u K_1 = \Delta^s K_1$, is necessary for a nontrivial intersection $W^u(P_-) \cap W^s(P_-)$. At leading order in ε this takes the form

$$\int_{\mathbb{R}} \dot{u}_0 v_0 dr + \frac{1}{2}(D_0^u + D_0^s)\int_{\mathbb{R}} \dot{u}_0^2 dr = \frac{1}{2}(D_0^u + D_0^s)\int_{\mathbb{R}} \dot{u}_0^2 dr = 0. \qquad (3.20)$$

Similarly, it follows from $\Delta^u K_2 = \Delta^s K_2$ that,

$$\frac{1}{2}(D_0^u + D_0^s)\int_{\mathbb{R}} \left[\ddot{u}_0 v_0 + \dot{u}_0 \dot{v}_0 - \eta_1 \dot{u}_0^2\right] dr - \frac{\alpha}{R_0}\int_{\mathbb{R}} \left[2\dot{u}_0 \dot{v}_0 + \eta_1 \dot{u}_0^2\right] dr = 0. \qquad (3.21)$$

The combination of (3.20) and (3.21) yields existence condition (3.13) and a first condition on the parameters $D_0^{u,s}$: $D_0^s + D_0^u = 0$. Naturally, one would expect to deduce a second condition on $D_0^{u,s}$ by the application of the third Melnikov condition $\Delta^u H = \Delta^s H$, which would yield the homoclinic orbit $\Gamma_h(r)$, uniquely determined by (3.13). However, this condition only reconfirms (3.13). This is caused by our choice to measure the distance between $W^u(P_-)$ and $W^s(P_-)$ as they intersect the $\{p = 0\}$-hyperplane. Based on the dynamics of (3.4), this is a very natural choice, however, the level sets of $K_{1,2}$ and H degenerate in $\{p = 0\}$. More specifically, q drops out of K_2 and H when $p = 0$ (and $K_1 = K_1(u, p)$) – see (3.9), (3.7).

There are two natural ways to repair this technical inconvenience: one is to measure the distance between $W^u(P_-)$ and $W^s(P_-)$ in another hyperplane, the second is to study the evolution of the q-components of orbits in $W^{u,s}(P_-)$ independently. The former approach generates extended, but straightforward, calculations since we cannot exploit the fact that v_0 and v_0 are even as function of r. The latter approach works smoothly since $\Delta^u q$ and $\Delta^s q$ can be approximated by (3.19) (and (3.4)). Pursuing the latter argument, it follows from the relation $\Delta^u q = \Delta^s q$ that,

$$D_0^u \int_{-\infty}^0 W''(u_0)\dot{u}_0 dr + D_0^s \int_0^\infty W''(u_0)\dot{u}_0 dr = (D_0^u - D_0^s)W'(u_0(0)) = 0, \qquad (3.22)$$

where we used the homoclinic limits $\lim_{r \to \pm\infty} W'(u_0(r)) = W'(-1) = 0$. Since $-1 < u_0(0) < m$ and $W'(u)$ has precisely 3 zeroes, it follows that $D_0^u - D_0^s = 0$ and we deduce from (3.20) that $D_0^u = D_0^s = 0$. We conclude that $W^u(P_-)$ and $W^s(P_-)$ intersect transversally when (3.13) holds, and that the homoclinic orbit $\Gamma_h(r) = W^u(P_-) \cap W^s(P_-)$ agrees with Γ_0 at leading order, establishing Theorem 3.1.

Apart from the reversibility of $\Gamma_h(r)$, the proof of Corollary 3.2 for the Hamiltonian system (3.6) follows directly from (3.20), (3.21) and (3.22) – where it should be noted that coefficient, α, of existence condition (3.13) is zero and this condition disappears from (3.21). Since the flat system (3.6) is reversible, a non-reversible orbit $\Gamma_h(r)$ would yield the existence of a second homoclinic orbit. However the leading order approximation $\Gamma_0(r)$ is reversible, and the distance between the two distinct intersections $W^u(P_-) \cap W^s(P_-)$ will be $\ll \varepsilon$. Moreover, both $\dot{K}_{1,2}$ are $\mathcal{O}(\varepsilon)$ (3.10), so that the manifolds $W^u(P_-)$ and $W^s(P_-)$ intersect with an $\mathcal{O}(\varepsilon)$ angle (and not smaller than $\mathcal{O}(\varepsilon)$): $W^u(P_-)$ and $W^s(P_-)$ cannot have two such intersections. Thus, $\Gamma_h(r)$ must be reversible. $\square$

Theorem 3.1 and Corollary 3.2 address the existence of homoclinic solutions, $\Gamma_h(r; \alpha)$ of (3.4) posed on $\mathbb{R}$. For a domain Ω which shares of the α-symmetry, the local coordinate system in fact foliates the whole domain; that is $r = r(x)$ for all $x \in \Omega$. Consequently we may define functions $U_h(x; \alpha) := u_h(r; \alpha)$ on Ω which solve (3.1), except for the homogeneous Neumann boundary conditions at $r = R_b/\varepsilon$ and the singularity at the caustic K-dimensional surface $r = -R_0/\varepsilon$. However, since u_h decays exponentially in $|r|$, and u_h is approximately constant in these regions a solution that is exponentially close to U_h can be constructed that does satisfy the boundary conditions and is smooth at the center $r = -R_0/\varepsilon$ (see [10] for a detailed treatment of a similar issue). As a consequence, for a given $R_b = \mathcal{O}(1) > 0$, there is a solution $\Gamma_{h,b}(r) = (u_{h,b}(r), p_{h,b}(r), v_{h,b}(r), q_{h,b}(r))$ of (3.4), defined on the interval $[-\frac{R_0}{\varepsilon}, \frac{R_b}{\varepsilon}]$, that is exponentially close to $\Gamma_h(r)$ and that satisfies the boundary conditions,

$$\dot{u}_{h,b}(R_b/\varepsilon) = p_{h,b}(R_b/\varepsilon) = 0, \quad \dot{v}_{h,b}(R_b/\varepsilon) = q_{h,b}(R_b/\varepsilon) = 0,$$

In particular the "dressing" $U_{h,b}(x) := u_{h,b}(r(x))$ of the interface $\{x \mid r(x) = 0\}$ with $u_{h,b}$ solves (3.1) in all of Ω, including at $r = -R_0/\varepsilon$, as well as satisfying the homogeneous Neumann conditions on $\partial\Omega$. This establishes the following Corollary.

COROLLARY 3.3. *Fix $\eta_d, \eta_1 = \mathcal{O}(1) \in \mathbb{R}$ and $R_0 \in (0, R_b)$ with R_0 and $R_b - R_0$ sufficiently large. Let $W(u)$ be a non-degenerate double-well potential and let ε be sufficiently small. For $\alpha > 0$, let $\gamma_h = \gamma_h(\varepsilon)$ be as in Theorem 3.1, and let Ω share the α symmetry. Then there exists $U_{h,b} \in H^4(\Omega)$, defined through $\Gamma_{h,b}$, which solves (3.1) on all of Ω, and satisfies the homogeneous Neumann boundary conditions. Moreover $U_{h,b}$ is exponentially close in $H^4(\Omega)$ to U_h, which is defined in terms of Γ_h. For the flat case, $\alpha = 0$, the existence result hold without restriction on $\gamma = \mathcal{O}(1)$.*

In the forthcoming stability analysis we will not distinguish between $U_{h,b}$ and U_h.

3.3. Higher-order accuracy. As is common in the study of localized structures, the stability analysis requires more details about the existence problem than the existence theorem itself. More specifically, in section 4.4 we will need a more accurate resolution of the existence condition (3.13), and higher order approximations of the $u_h(r)$ and $v_h(r)$ components of the homoclinic orbit $\Gamma_h(r)$. To this end we introduce the expansions,

$$
\begin{aligned}
u_h(r) &= u_0(r) + \varepsilon u_1(r) + \varepsilon^2 u_2(r) + \varepsilon^3 u_3(r) + \mathcal{O}(\varepsilon^4), \\
v_h(r) &= v_0(r) + \varepsilon v_1(r) + \varepsilon^2 v_2(r) + \varepsilon^3 v_3(r) + \mathcal{O}(\varepsilon^4),
\end{aligned}
\tag{3.23}
$$

where u_0 and v_0 were previously defined in (3.8) and (3.12) respectively. Substituting the expansions into (3.4) and collecting terms at order of $\varepsilon, \varepsilon^2$, and ε^3 yields the relations,

$$
\begin{aligned}
\mathcal{L}u_1 &= v_0, \\
\mathcal{L}v_1 &= \left[\gamma_2 + \frac{\alpha(2-\alpha)}{R_0^2} W'(u_0) - \eta_1 v_0\right] - \frac{\alpha}{R_0}\left[2\dot{v}_0 + \eta_1 \dot{u}_0\right] + u_1 v_0 W'''(u_0) - \eta_d u_1 W''(u_0), \\
\mathcal{L}u_2 &= v_1 + \tfrac{1}{2}u_1^2 W'''(u_0).
\end{aligned}
\tag{3.24}
$$

The function v_0, and hence u_1, is even in z, the other inhomogeneities contain both odd and even functions. Moreover in the $\alpha = 0$ case all terms are even; by inspection we remark that α/R_0 may be factored out of the odd components. This observation motivates the decomposition,

$$
v_j = v_{j,e} + \frac{\alpha}{R_0}\tilde{v}_{j,o}, \quad u_{j+1} = u_{j+1,e} + \frac{\alpha}{R_0}\tilde{u}_{j+1,o}, \quad j = 1, 2, 3, ...,
\tag{3.25}
$$

into even and odd functions. Since $\mathcal{L}$ preserves parity, we have the relations

$$
\mathcal{L}\tilde{v}_{1,o} = -\left[2\dot{v}_0 + \eta_1 \dot{u}_0\right], \quad \mathcal{L}\tilde{u}_{2,o} = \tilde{v}_{1,o}.
\tag{3.26}
$$

Each of the elements of the expansion converge exponentially to a constant value as $r \to \pm\infty$, with the odd elements converging to zero. We denote these limiting values by u_j^∞ or v_j^∞ respectively. Since u_0 is homoclinic to the left well of W, we have $u_0^\infty = -1$; while from (3.11), (3.12), (3.24), and the relations $W'(-1) = 0$, $W''(-1) = \mu_1 > 0$ it follows that

$$
v_0^\infty = -\frac{\gamma_1}{\mu_-}, \quad u_1^\infty = \frac{\gamma_1}{\mu_-^2},
\tag{3.27}
$$

in agreement with (3.5).

REMARK 3.4. *Since the range of $\mathcal{G}$ is orthogonal to the constants, the total mass, $\langle u, 1 \rangle_\Omega$ of a solution u of (1.4) is conserved under the flow. The mass of the solution U_h obtained by dressing Γ with u_h depends, at leading order, in equal measure upon background state u_1^∞ and the $d-1$ dimensional surface area, $|\Gamma| = m_\alpha R_0^\alpha \Pi_{j=1}^K L_j$, of Γ, where m_α is the surface area of S_α. Indeed via (2.10) and (3.17) we have the relation*

$$
\langle U_h, 1 \rangle_\Omega = \varepsilon\left(|\Omega|u_1^\infty + |\Gamma|M_0\right) + O(\varepsilon^2) = \varepsilon\left(\frac{|\Omega|\gamma_1}{\mu_-^2} + |\Gamma|M_0\right) + O(\varepsilon^2).
\tag{3.28}
$$

In particular, the total mass of U_h determines the value of R_0.

We work directly with the fourth-order system (3.1) to derive the higher-order existence condition. Substitution of (3.23) into (3.1), expanding $W'(u_h)$, $W''(u_h)$, and using (3.3), (3.8), and (3.11) yields

$$
\begin{aligned}
&\left\{\mathcal{L} + \varepsilon\left[\frac{\alpha}{R_0}\partial_r - u_1 W'''(u_0) + \eta_1\right] + \varepsilon^2 \mathcal{P}_2\right\}\left\{\varepsilon\left[\mathcal{L}u_1 + \frac{\alpha}{R_0}\dot{u}_0\right] + \varepsilon^2 \mathcal{Q}_2 + \varepsilon^3 \mathcal{Q}_3\right\} \\
&+ \varepsilon\eta_d W'(u_0) + \varepsilon^2 \eta_d u_1 W''(u_0) + \varepsilon^3 \eta_d\left[u_2 W''(u_0) + \tfrac{1}{2}u_1^2 W'''(u_0)\right] \\
&\qquad = \varepsilon\gamma_1 + \varepsilon^2\gamma_2 + \varepsilon^3\gamma_3 + \mathcal{O}(\varepsilon^4),
\end{aligned}
\tag{3.29}
$$

where we have introduced the operator

$$\mathcal{P}_2 := -\frac{\alpha}{R_0^2} r \partial_r - u_2 W'''(u_0) - \frac{1}{2} u_1^2 W''''(u_0), \tag{3.30}$$

and the residual

$$\mathcal{Q}_2 := \mathcal{L} u_2 + \frac{\alpha}{R_0} \dot{u}_1 - \frac{\alpha}{R_0^2} r \dot{u}_0 - \frac{1}{2} u_1^2 W'''(u_0). \tag{3.31}$$

Similarly, an expression can be determined for $\mathcal{Q}_3$. Collecting terms at $\mathcal{O}(\varepsilon)$ yields,

$$\mathcal{L}^2 u_1 = \gamma_1 - \eta_d W'(u_0) - \frac{\alpha}{R_0} \mathcal{L} \dot{u}_0.$$

It is easy to verify that the right-hand side is orthogonal to $\ker(\mathcal{L}) = \mathrm{span}\{\dot{u}_0\}$ and hence in the range of $\mathcal{L}$. Inverting $\mathcal{L}^2$, we solve for u_1. At $\mathcal{O}(\varepsilon^2)$ we find,

$$\mathcal{L} \mathcal{Q}_2 = \gamma_2 - \left(\frac{\alpha}{R_0} \partial_r - u_1 W'''(u_0) + \eta_1 \right) \left(\mathcal{L} u_1 + \frac{\alpha}{R_0} \dot{u}_0 \right) - \eta_d u_1 W''(u_0).$$

Since u_0 and u_1 are even, the existence condition for u_2 reduces to

$$\langle \partial_r \mathcal{L} u_1 + (\eta_1 - u_1 W'''(u_0)) \dot{u}_0, \dot{u}_0 \rangle = 0, \tag{3.32}$$

where we have factored out the term $\frac{\alpha}{R_0}$. For any smooth, bounded $\phi : \mathbb{R} \to \mathbb{R}$,

$$\partial_r \mathcal{L} \phi = \mathcal{L} \dot{\phi} - \phi W'''(u_0) \dot{u}_0, \tag{3.33}$$

and hence, taking $\phi = u_1$, and substituting the result into (3.32), the existence condition reduces to

$$\eta_1 \| \dot{u}_0 \|_2^2 = 2 \langle u_1, W'''(u_0) \dot{u}_0^2 \rangle. \tag{3.34}$$

Moreover (3.33) with $\phi = \dot{u}_0$, together with (3.24), implies that

$$\langle u_1, W'''(u_0) \dot{u}_0^2 \rangle = \langle u_1, \mathcal{L} \ddot{u}_0 \rangle = \langle \mathcal{L} u_1, \ddot{u}_0 \rangle = \langle v_0, \ddot{u}_0 \rangle = -\langle \dot{v}_0, \dot{u}_0 \rangle,$$

so that (3.34) is equivalent to (3.13). A similar but more involved analysis at the $\mathcal{O}(\varepsilon^3)$ level yields the higher-order existence condition.

LEMMA 3.5. *Under the assumptions of Theorem 3.1, for any $\alpha > 0$, the higher-order existence condition takes the form,*

$$\eta_1 \langle \dot{u}_1, \dot{u}_0 \rangle - \langle 2 u_1 \dot{u}_1 W'''(u_0) + 2 \dot{u}_0 u_2 W'''(u_0) + \dot{u}_0 u_1^2 W''''(u_0), \dot{u}_0 \rangle = \langle 2 \dot{v}_0 + \eta_1 \dot{u}_0, \dot{u}_1 \rangle, \tag{3.35}$$

in terms of the elements of the expansion (3.23) of u_h and v_h (3.25).

Proof. Equating terms at $\mathcal{O}(\varepsilon^3)$ in (3.29) yields the equality

$$\mathcal{L} \mathcal{Q}_3 = \gamma_3 - \left[\frac{\alpha}{R_0} \partial_r - u_1 W'''(u_0) + \eta_1 \right] \mathcal{Q}_2 - \mathcal{P}_2 \left[\mathcal{L} u_1 + \frac{\alpha}{R_0} \dot{u}_0 \right] - \eta_d \left[u_2 W''(u_0) + \frac{1}{2} u_1^2 W'''(u_0) \right],$$

where $\mathcal{Q}_3$ contains the unknown u_3 in the form $\mathcal{L} u_3$. Inverting $\mathcal{L}$ requires the right-hand side to be orthogonal to its kernel. Taking the inner product with $\dot{u}_0$, applying (3.33) with various choices of ϕ, using (3.25), (3.26), and factoring out $\frac{\alpha}{R_0}$, the existence condition becomes

$$\eta_1 \langle \dot{u}_1, \dot{u}_0 \rangle - \langle 2 u_1 \dot{u}_1 W'''(u_0) + 2 \dot{u}_0 u_2 W'''(u_0) + u_1^2 \dot{u}_0 W''''(u_0), \dot{u}_0 \rangle$$
$$= \langle \eta_d \tilde{u}_{2,o} W''(u_0), \dot{u}_0 \rangle - \langle W'''(u_0) [u_1 \mathcal{L} \tilde{u}_{2,o} + \tilde{u}_{2,o} \mathcal{L} u_1], \dot{u}_0 \rangle.$$

Using (3.33) the second term on the right-hand side can be written as

$$\langle W'''(u_0) [u_1 \mathcal{L} \tilde{u}_{2,o} + \tilde{u}_{2,o} \mathcal{L} u_1], \dot{u}_0 \rangle = \int_{\mathbb{R}} \left\{ \mathcal{L} \tilde{u}_{2,o} [\mathcal{L} \dot{u}_1 - \partial_r \mathcal{L} u_1] + \mathcal{L} u_1 [\mathcal{L} \dot{\tilde{u}}_{2,o} - \partial_r \mathcal{L} \tilde{u}_{2,o}] \right\} dr,$$
$$= \int_{\mathbb{R}} \left[\dot{u}_1 \mathcal{L}^2 \tilde{u}_{2,o} + \dot{\tilde{u}}_{2,o} \mathcal{L}^2 u_1 \right] dr - \int_{\mathbb{R}} \partial_r \left[(\mathcal{L} u_1)(\mathcal{L} \tilde{u}_{2,o}) \right] dr.$$

Using the relations (3.24), (3.26), and (3.27) we find

$$\langle W'''(u_0) [u_1 \mathcal{L} \tilde{u}_{2,o} + \tilde{u}_{2,o} \mathcal{L} u_1], \dot{u}_0 \rangle = \int_{\mathbb{R}} \left[\dot{u}_1 \mathcal{L} \tilde{v}_{1,o} + \dot{\tilde{u}}_{2,o} \mathcal{L} v_0 \right] dr - [v_0 v_{1,o}]_{-\infty}^{\infty},$$
$$= \int_{\mathbb{R}} \left\{ -\dot{u}_1 [2 \dot{v}_0 + \eta_1 \dot{u}_0] + \dot{\tilde{u}}_{2,o} [\gamma_1 - \eta_d W'(u_0)] \right\} dr,$$
$$= -\langle 2 \dot{v}_0 + \eta_1 \dot{u}_0, \dot{u}_1 \rangle + \eta_d \int_{\mathbb{R}} \tilde{u}_{2,o} W''(u_0) \dot{u}_0 \, dr,$$

which recovers (3.35). $\square$

4. Spectral stability. In this section we address the linear stability of an α-single curvature bilayer morphology, $U_h(x; \alpha)$, formed by dressing an α-single curvature interface Γ with the homoclinic profile $u_h(x; \alpha)$. We consider general perturbations of U, and decompose the solution u of (1.4) as

$$u(x, t) = U_h(x; \alpha) + v(x, t), \tag{4.1}$$

up to exponentially small terms (see Corollary 3.3), and linearize (1.4) in v, obtaining the flow

$$v_t = -\mathcal{G}\mathbb{L}v.$$

The gradient $\mathcal{G}$ is as described in the introduction, while $\mathbb{L}(\alpha) := \frac{\delta^2 \mathcal{F}}{\delta u^2}(U_h)$, the second variation of the FCH energy at U_h, takes the form

$$\mathbb{L} = \left(\varepsilon^2 \Delta - W''(U_h) + \varepsilon \eta_1\right) \left(\varepsilon^2 \Delta - W''(U_h)\right) - \left(\varepsilon^2 \Delta U_h - W'(U_h)\right) W'''(U_h) + \varepsilon \eta_d W''(U_h). \tag{4.2}$$

As is illustrated in (4.22), and formulated rigorously in [9], the eigenvalues of $\mathbb{L}$ which are potentially unstable are at most $O(\varepsilon)$ in magnitude. Indeed, as the next Lemma shows, any bifurcations in the spectrum of the operator $-\mathcal{G}\mathbb{L}$ are independent of the choice of gradient $\mathcal{G}$. In particular a sharp characterization of the sign of the non-zero spectrum of $-\mathcal{G}\mathbb{L}$ can be obtained from a study of the operator $\mathbb{L}_0 := \Pi_0 \mathbb{L}$, which corresponds to choice of the simplest admissible gradient $\mathcal{G} = \Pi_0$, defined in (1.5).

LEMMA 4.1. *The spectrum of $\mathcal{G}\mathbb{L}$ is real, with $\ker(\mathcal{G}\mathbb{L}) = \ker(\mathbb{L}) \cup \{\mathbb{L}^{-1}1\}$. The set $\sigma(-\mathcal{G}\mathbb{L})\backslash\{0\}$ is negative if and only if the set $\sigma(\mathbb{L}_0)\backslash\{0\}$ is positive. Moreover if for some $\nu > 0$ we have $\sigma(\mathbb{L}_0)\backslash\{0\} \subset [\nu, \infty)$, then $\sigma(-\mathcal{G}\mathbb{L})\backslash\{0\} \subset (-\infty, -C_1\nu])$ where the constant*

$$C_1 := \inf_{u \perp 1} \frac{\langle \mathcal{G}u, u \rangle_\Omega}{\|u\|_{L^2_\Omega}^2} > 0, \tag{4.3}$$

is independent of ε.

Proof. From the eigenvalue problem

$$-\mathcal{G}\mathbb{L}\Psi = \lambda\Psi, \tag{4.4}$$

we deduce that either $\lambda = 0$ or Ψ is in the range of $\mathcal{G}$ and hence orthogonal to the constants. The kernel of $\mathcal{G}\mathbb{L}$ is formed of the kernel of $\mathbb{L}$, combined with $\mathbb{L}^{-1}1$, if it exists. For $\lambda \neq 0$, we have the identity

$$\lambda = -\frac{\langle \mathbb{L}\Psi, \Psi \rangle_\Omega}{\|\mathcal{G}^{-\frac{1}{2}}\Psi\|_{L^2_\Omega}^2} \leq -C_1 \frac{\langle \mathbb{L}\Psi, \Psi \rangle_\Omega}{\|\Psi\|_{L^2_\Omega}^2}, \tag{4.5}$$

where the inequality follows from the coercivity of $\mathcal{G}$, (4.3). In particular there exists $\nu > 0$ such that $\sigma(-\mathcal{G}\mathbb{L})\backslash\{0\} \subset (-\infty, -\nu]$ only if $\sigma(\mathbb{L}_0)\backslash\{0\} \subset [\frac{\nu}{C_1}, \infty)$, where $\mathbb{L}_0 := \Pi_0 \mathbb{L}$ is the operator generated by the bilinear form

$$b[u, v] := \langle \mathbb{L}u, v \rangle_\Omega, \tag{4.6}$$

constrained to act on $u, v \in \mathcal{A} := \mathcal{R}(\Pi_0) \cap H^2(\Omega)$. Conversely, suppose that $-\mathcal{G}\mathbb{L}$ has a positive eigenvalue λ, then from (4.5) we know that $\mathbb{L}_0$ has a non-trivial negative space, and hence a negative eigenvalue. $\qquad\square$

The operator $\mathbb{L}_0$ is obtained from $\mathbb{L}$ by a rank-one constraint. Let $n(\mathbb{L})$ denote the dimension of the negative eigenspaces of a self-adjoint operator $\mathbb{L}$, in particular for a scalar, $r \in \mathbb{R}$, $n(r) = 1$ if $r < 0$ and 1 if $r \geq 0$. The following result is a consequence of Proposition 5.3.1 and Theorem 5.3.5 of [13], see also [12].

LEMMA 4.2. *The negative eigenvalue count of $\mathbb{L}$ and $\mathbb{L}_0$ are related by*

$$n(\mathbb{L}_0) = n(\mathbb{L}) - n(\langle \mathbb{L}^{-1}1, 1 \rangle), \tag{4.7}$$

moreover the set $\sigma(\mathbb{L}_0)$ lies strictly to the right of the set $\sigma(\mathbb{L})$ in the sense that the i'th eigenvalue of $\mathbb{L}_0$ lies to the right of the i'th eigenvalue of $\mathbb{L}$, each counted according to multiplicity.

These two Lemmas show that bifurcations of U_h, that is crossing of eigenvalues of $-\mathcal{G}\mathbb{L}$ through zero, can be identified via the spectrum of $\mathbb{L}$.

4.1. Invariant subspaces for $\mathbb{L}$. A perturbation analysis of the spectrum of $\mathbb{L}$ is potentially complicated by the fact that its eigenvalues are asymptotically close together, and coupling between eigenspaces could potentially disrupt the asymptotic order. However we show that the operator $\mathbb{L}$ possesses a large family of invariant subspaces which remain invariant for the approximations of $\mathbb{L}$ we consider. Moreover the spectrum of $\mathbb{L}$ restricted to any particular subspace is well-separated, and can be uniformly approximated. On Ω, the eigenfunctions Ψ of $\mathbb{L}$ admit a separated variables decomposition

$$\Psi_{jkl}(x) = \mathcal{T}_j(\tau)\Theta_k(\theta)\psi_l(r), \tag{4.8}$$

where $\{\mathcal{T}_j\}_{j=0}^{\infty}$ and $\{\Theta_k\}_{k=0}^{\infty}$ are eigenfunctions of Δ_τ and Δ_θ respectively, see (2.7), satisfying

$$\Delta_\tau \mathcal{T}_j = -\mu_j \mathcal{T}_j, \qquad \text{and} \qquad \Delta_\theta \Theta_k = -\nu_k \Theta_k, \tag{4.9}$$

subject to Neumann boundary conditions for Δ_τ and periodic boundary conditions for Δ_θ. The eigenvalues μ_j and ν_k are non-negative and non-decreasing in their index. For the case of the sphere in $\mathbb{R}^3$, with $\alpha = 2$, we have $\mathcal{T} \equiv 1$ and $\Theta = \Theta(\theta_1, \theta_2)$ is a spherical harmonic

$$\Theta_k(\theta) = e^{im\theta_1} P_\ell^m(\theta_2), \tag{4.10}$$

with $\theta_1 \in [0, 2\pi)$, $\theta_2 \in [0, \pi)$, $m \in \mathbb{Z} \cap [-\ell, \ell]$, and $P_\ell^m(\theta_2)$ is the Legendre polynomial, i.e. a bounded solution of the Legendre equation,

$$P_{\theta_2\theta_2} + \frac{\cos\theta_2}{\sin\theta_2} P_{\theta_2} + \left[\ell(\ell+1) - \frac{m^2}{\sin^2\theta_2}\right] P = 0,$$

with $\ell = 0, 1, 2, ...$ and $k = k(l, m)$. In particular, since there are no straight directions we take $\mu_j = 0$, while for $\ell = 0$ we have $\nu_0 = 0$, for $\ell = 1$ we have $\nu_1 = \nu_2 = 2$, corresponding to $m = -1, 1$, while $\nu_k > 2$ for $k \geq 3$, see [18] for details. Similarly, cylindrical coordinates in $\mathbb{R}^3$ correspond to $\alpha = 1$ for which $\tau = \tau_1 \in [0, L)$, $\theta = \theta_1 \in [0, 2\pi)$, while

$$\mathcal{T}_j(\tau) = e^{\frac{\pi ij}{L}\tau} \qquad \text{and} \qquad \Theta_k(\theta) = e^{ik\theta}, \tag{4.11}$$

where L denotes the length of the cylinder in the t direction. Here $\mu_j = \frac{\pi^2 j^2}{L^2}$, for $j = 0, 1, \ldots$, and $\nu_k = k^2$ for $k \in \mathbb{Z}_+$. For the general α-single curvature interface we have $\mu_0 = 0$ while μ_j is the $j+1$'st smallest element of the set

$$\left\{\pi^2 \sum_{j=1}^{K} \left(\frac{n_j}{L_j}\right)^2 \,\Big|\, (n_1, \ldots, n_k) \in \mathbb{Z}_+^K\right\}. \tag{4.12}$$

In particular, if L_1 is the largest length, then $\mu_1 = \pi^2/L_1^2 > 0$. On the other hand, the Laplace-Beltrami eigenmodes of S_α satisfy $\nu_0 = 0$ and $\nu_1 = \cdots = \nu_\alpha = \alpha$, with $\nu_{\alpha+1} > \alpha$.

Crucially, through (2.7), the action of Δ on $\Psi = \mathcal{T}_j\Theta_k\psi_l$ takes the form

$$\varepsilon^2 \Delta\Psi = \mathcal{T}_j\Theta_k \left(\partial_r^2 + \varepsilon\kappa(r)\partial_r - \varepsilon^2\beta(r; j, k)\right)\psi_l,$$

where we have introduced the potential

$$\beta(r; j, k) := \mu_j + \frac{\nu_k}{(R_0 + \varepsilon r)^2}. \tag{4.13}$$

Consequently the action of $\mathbb{L}$ maps the spaces

$$\mathcal{Z}_{jk} := \{Z(r)\mathcal{T}_j(\tau)\Theta_k(\theta) \big| Z \in \mathcal{C}^\infty(\mathbb{R})\}, \tag{4.14}$$

into themselves, and its eigenvalue problem may be considered on each invariant subspace separately, on which the operator takes the single-variable, fourth-order form

$$\begin{aligned}
\mathbb{L}_{jk} \quad := \quad & \left[(\partial_r^2 - W''(u_h)) + \varepsilon(\kappa\partial_r + \eta_1) - \varepsilon^2\beta\right] \circ \left[(\partial_r^2 - W''(u_h)) + \varepsilon\kappa\partial_r - \varepsilon^2\beta\right] \\
& - \left[(\ddot{u}_h - W'(u_h)) + \varepsilon\kappa\dot{u}_h - \varepsilon^2\beta u_h\right] W'''(u_h) + \varepsilon\eta_d W''(u_h).
\end{aligned} \tag{4.15}$$

To elucidate the structure of $\mathbb{L}$ we expand $\kappa = \kappa(r; \varepsilon)$ and $\beta = \beta(r; \varepsilon, j, k)$,

$$
\begin{aligned}
\beta(r; j, k) &= \mu_j + \frac{\nu_k}{R_0^2} - \varepsilon r \frac{2\nu_k}{R_0^3} + O(\varepsilon^2 r^2 \nu_k) = \beta_0(j, k) - 2\varepsilon \frac{r}{R_0}\beta_1(j, k) + O(\varepsilon^2 r^2 \nu_k), \\
\kappa &= \frac{\alpha}{R_0} - \varepsilon r \frac{\alpha}{R_0^2} + O(\varepsilon^2 r^2),
\end{aligned}
\tag{4.16}
$$

where we have introduced $\beta_0(j, k) := \mu_j + \nu_k/R_0^2$, and $\beta_i(j, k) = \nu_k/R_0^2$ for $i \geq 1$. We insert the expansions, (3.23), of u_h and v_h into $\mathbb{L}$, and recalling the definition, (3.11), of $\mathcal{L}$ we obtain

$$
\begin{aligned}
\mathbb{L}_{jk} &= \left[(\mathcal{L} - \varepsilon^2 \beta_0) + \varepsilon \left(\frac{\alpha}{R_0}\partial_r + \eta_1 - W'''(u_0)u_1 + \varepsilon^2 2\beta_1 \frac{r}{R_0} \right) + \mathcal{O}(\varepsilon^2) \right] \circ \\
&\quad \left[(\mathcal{L} - \varepsilon^2 \beta_0) + \varepsilon \left(\frac{\alpha}{R_0}\partial_r - W'''(u_0)u_1 + \varepsilon^2 2\beta_1 \frac{r}{R_0} \right) + \mathcal{O}(\varepsilon^2) \right] + \\
&\quad \varepsilon \left[\eta_d W''(u_0) - (v_0 + \frac{\alpha}{R_0}\dot{u}_0)W'''(u_0) \right] + \mathcal{O}(\varepsilon^2),
\end{aligned}
\tag{4.17}
$$

where $\varepsilon^2 \beta_0$ is grouped with the $O(1)$ terms since β_0 is potentially large for large values of index (j, k). Collecting orders of ε, we obtain the expansion

$$
\begin{aligned}
\mathbb{L}_{jk} &= (\mathcal{L} - \varepsilon^2 \beta_0)^2 + \varepsilon \Big[(\mathcal{L} - \varepsilon^2 \beta_0)\mathcal{P}_1 + (\mathcal{P}_1 + \eta_1)(\mathcal{L} - \varepsilon^2 \beta_0) + \\
&\quad \Big(\eta_d W''(u_0) - (v_0 + \frac{\alpha}{R_0}\dot{u}_0)W'''(u_0) \Big) \Big] + O(\varepsilon^2),
\end{aligned}
\tag{4.18}
$$

where we have introduced the operator $\mathcal{P}_1 := \frac{\alpha}{R_0}\partial_r - W'''(u_0)u_1 + \varepsilon^2 \beta_1 r/R_0$. The dominant term in $\mathbb{L}_{jk}$ is strictly positive, and since $\beta_0 > 0$ the dominant term can be small only on subspaces where $\mathcal{L}$ is positive. However $\mathcal{L}$ is a Sturm-Liouville/Schrödinger operator, and from classical considerations, see [23], it is known that the eigenvalue problem,

$$
\mathcal{L}\psi_j = \lambda_j \psi_j,
\tag{4.19}
$$

has $J \geq 2$ simple eigenvalues $\{\lambda_j\}_{j=0}^{J-1}$ with $\lambda_0 > 0$, $\lambda_1 = 0$, and the remainder strictly negative. In particular the ground-state eigenfunction $\psi_0 > 0$ has no zeros, while the translational eigenfunction, $\psi_1 = \dot{u}_0$, spans the kernel of $\mathcal{L}$. Thus the dominant term of $\mathbb{L}_{jk}$ can vanish, at least to $O(\varepsilon)$, precisely under two situations – see Figure 4.2. The first is when it acts on $\psi_1 = \dot{u}_0$, and the indices lie in

$$
\mathcal{I}_m := \left\{ (j, k) \in \mathbb{Z}_+^2 \,\big|\, \beta_0(j, k) = \mathcal{O}(\varepsilon^{-3/2}) \right\}
\tag{4.20}
$$

In this case

$$
\left(\mathcal{L} - \varepsilon^2 \beta_0 \right)^2 \psi_1 = \left(\lambda_1 - \varepsilon^2 \beta_0 \right)^2 \psi_1 = \varepsilon^4 \beta_0^2 \psi_1 = O(\varepsilon).
$$

The second case is when $\mathbb{L}_{jk}$ acts on the ground state, ψ_0, and the indices lie in

$$
\mathcal{I}_p := \left\{ (j, k) \in \mathbb{Z}^2 \,\big|\, |\beta_0(j, k) - \lambda_0 \varepsilon^{-2}| = \mathcal{O}(\varepsilon^{-3/2}) \right\},
\tag{4.21}
$$

for which

$$
\left(\mathcal{L} - \varepsilon^2 \beta_0 \right)^2 \psi_0 = \left(\lambda_0 - \varepsilon^2 \beta_0 \right)^2 \psi_1 = O(\varepsilon).
\tag{4.22}
$$

The former case, in which relatively long-wavelength perturbations of the front location drive a linear instability of the front shape, is called the *meander instability*. The latter case, in which the front width may become unstable to relatively short-wavelength in-plane perturbations, is called the *pearling instability*. Indeed there exists $\overline{\sigma} > 0$, independent of (j, k) and $\varepsilon > 0$ such that

$$
(\sigma(\mathbb{L}_{jk}) \cap (-\infty, \overline{\sigma}]) \subset \{\Lambda_m(j, k), \Lambda_p(j, k)\},
\tag{4.23}
$$

where the meander eigenvalue, Λ_m, is associated with eigenfunction $\psi_m(r; j, k) = \dot{u}_0 + O(\varepsilon)$ and the pearling eigenvalue Λ_p is associated with eigenfunction $\psi_p(r; j, k) = \psi_0(r) + \mathcal{O}(\varepsilon)$.
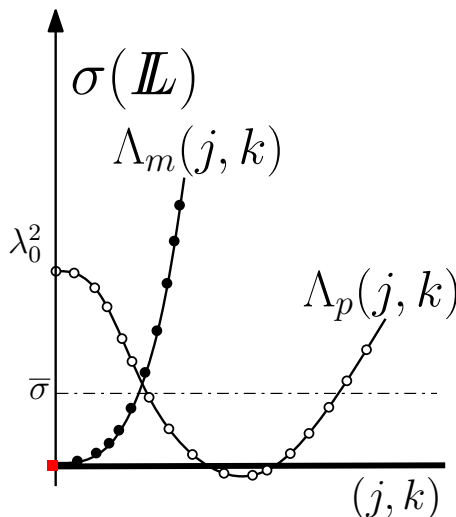
FIG. 4.1. *Depiction of the real meander (closed circles) and pearling (open circles) point spectrum* $\{\Lambda_m(j,k), \Lambda_p(j,k)\}$ *of* $\mathbb{L}$ *as function of index* (j,k) *when the pearling stability condition, (4.32) is violated. The meander eigenvalues are* $\mathcal{O}(\varepsilon^4)$ *for* (j,k) *sufficiently small, while the pearling eigenvalues are* $\mathcal{O}(\varepsilon)$ *for values of* $(j,k) \in \mathcal{I}_p$, *and are close to* λ_0^2 *for* (j,k) *small. The* $(0,0)$ *meander eigenvalue (red square) is typically negative, but is rendered positive by the mass constraint in* $\Pi_0 \mathbb{L}$, *see Lemma 4.8*

4.2. Proof of Theorem 1.2: Interim summary and strategy. From Lemma 4.1 we deduce that the spectrum of $-\mathcal{G}\mathbb{L}$, is contained on the strictly positive real axis if and only if the spectrum of $\mathbb{L}_0$ is. Moreover, the eigenfunctions $\{\mathcal{T}_j \Theta_k\}$ of $\Delta_\tau + \Delta_\theta$ are orthonormal with respect to the J_α-weighted inner product over $\hat{\Gamma}$, see (2.9),

$$\langle \mathcal{T}_{j_1} \Theta_{k_1}, \mathcal{T}_{j_2} \Theta_{k_2} \rangle_\Gamma := \int_{\hat{\Gamma}} \mathcal{T}_{j_1}(\tau) \Theta_{k_1}(\theta) \mathcal{T}_{j_2}(\tau) \Theta_{k_2}(\theta) J_\alpha(\theta) \, dt \, d\theta = \delta_{j_1 j_2} \delta_{k_1 k_2}, \tag{4.24}$$

where here δ_{ij} denotes the usual Kronecker delta. From the form, (2.6), of the $L^2(\Omega)$ inner product we deduce that the spaces $\mathcal{Z}_{j,k}$, defined in (4.14), are $L^2(\Omega)$ orthogonal to the function 1 for $(j,k) \neq (0,0)$, and hence these spaces are invariant under both Π_0 and $\mathbb{L}_0$. Thus, we may conclude that any eigenspace of $\mathbb{L}$ whose intersection with $\mathcal{Z}_{0,0}$ is trivial is an eigenspace of $\mathbb{L}_0$ with the same eigenvalue. As a consequence, to establish the linear stability of the α-single curvature bilayer U_h under the flow generated by a general admissible gradient $\mathcal{G}$ in (1.4), it is sufficient to study the spectrum of the operators $\mathbb{L}_{jk}$ (4.18) on the invariant spaces $\mathcal{Z}_{jk}$ (4.14) for $(j,k) \neq (0,0)$. Only for $(j,k) = (0,0)$ do we need to consider $\mathbb{L}_0$, and need never explicitly consider the full operator $-\mathcal{G}\mathbb{L}$. Moreover, from the coercivity estimates of Theorem 2.5 of [9], the meander and pearling eigenvalues are the only possible instability mechanisms – the remainder of the spectrum of $\mathbb{L}$ is strictly positive, as depicted in Figure 4.2.

The strategy of the proof of Theorem 1.2 follows this outline. In section 4.3, the pearling destabilization mechanism for curved, $\alpha > 0$, interfaces is considered. Its main result – Lemma 4.3 – establishes the pearling condition in the statement of the Theorem. The analysis of the meander instability for $\alpha > 0$ and $(j,k) \neq 0$ is presented in section 4.4. It is much more subtle than the pearling analysis. It is first shown in Lemma 4.4 that the magnitude of the eigenvalues must be asymptotically smaller than $\mathcal{O}(\varepsilon^3)$; Lemma 4.6 gives an exact $\mathcal{O}(\varepsilon^4)$ description of these eigenvalues. The interpretation of the asymptotic analysis is given in Corollary 4.7, that establishes the claims about the occurrence and non-occurrence of the meander instability in Theorem 1.2. The full statement of the Theorem follows from the analysis of the spectrum of $\mathbb{L}_0$ as it acts of $\mathcal{Z}_{0,0}$ in section 4.5. It shown in this section that this eigenvalue is positive and bounded from below by an $\mathcal{O}(\varepsilon^3)$ quantity, the quantitative statement in Theorem 1.2 about the existence of a constant $C_1 > 0$, independent of ε, such that $\sigma(-\mathcal{G}\mathbb{L})\backslash\{0\} \subset (-\infty, -C_1\varepsilon^4]$ also follows immediately.

Finally, we notice that the flat case, $\alpha = 0$, does not involve the solvability condition (3.13), and is therefore discussed separately in section 4.6.

4.3. The pearling eigenmodes. In this section we characterize the pearling eigenmodes, that is the eigenvalues of $\mathbb{L}_{jk}$ for $(j,k) \in \mathcal{I}_p$ corresponding at leading order to the eigenfucntion ψ_p. More specifically, we

consider an eigenfunction $\psi_p = \psi_p(r; j, k)$ and eigenvalue $\Lambda_p = \Lambda_p(j, k)$ of $\mathbb{L}_{jk}$, with expansions

$$\psi_p(r) = \psi_0 + \varepsilon\psi_{1,p} + \mathcal{O}(\varepsilon^2), \quad \Lambda_p = \varepsilon\Lambda_{1,p} + \varepsilon^2\Lambda_{2,p} + \mathcal{O}(\varepsilon^3). \tag{4.25}$$

We introduce $\tilde{\beta} = \varepsilon^2\beta$ and

$$\delta_0(j, k) := (\lambda_0 - \tilde{\beta}_0)\varepsilon^{-1/2} = O(1), \tag{4.26}$$

and substitute the expansions into the eigenvalue problem; using (4.18) we obtain

$$\begin{aligned}
\mathbb{L}_{jk}\psi_p &= \varepsilon(\mathcal{L} - \lambda_0)\psi_{1,p} + \varepsilon\left(\delta_0^2 + (\mathcal{L} - \lambda_0)\mathcal{P}_1 + (\mathcal{P}_1 + \eta_1)(\mathcal{L} - \lambda_0)\right)\psi_0 + \\
&\quad \varepsilon\left(\eta_d W''(u_0) - (v_0 + \tfrac{\alpha}{R_0}\dot{u}_0)W'''(u_0)\right)\psi_0 = \varepsilon\Lambda_{1,p}\psi_0 + \mathcal{O}(\varepsilon^{3/2}),
\end{aligned} \tag{4.27}$$

where we used $\tilde{\beta}_0 = \lambda_0 + O(\sqrt{\varepsilon})$. The solvability condition for $\psi_{1,p}$ requires the remaining terms be orthogonal to ψ_0, which spans the kernel of $\mathcal{L} - \lambda_0$. In particular the $\mathcal{P}_1$ and η_1 terms drop out and we are left with the expression for $\Lambda_{1,p}$,

$$\Lambda_{1,p}\|\psi_0\|_2^2 = \delta_0^2\|\psi_0\|_2^2 + \int_{\mathbb{R}}[\eta_d W''(u_0) - v_0 W'''(u_0)]\psi_0^2 dr,$$

where we have used that ψ_0, u_0, and v_0 are even in r while $\dot{u}_0$ is odd. Hence we may conclude that the pearling instability is uniquely controlled by the functionalization parameters η_1, η_2, and the shape of the double well potential, W, in particular through the "shape factor"

$$S := \int_{\mathbb{R}}\phi_1 W'''(u_0)\psi_0^2\, dr, \tag{4.28}$$

where we have introduced ϕ_1, the unique bounded solution to

$$\phi_1 := \mathcal{L}^{-1}1. \tag{4.29}$$

LEMMA 4.3. *Let the parameters satisfy the conditions formulated in Theorem 3.1, in particular $\alpha > 0$. Let u_h and v_h be expanded as in (3.23), let ψ_0 denote the ground-state eigenfunction of $\mathcal{L}$ with associated eigenvalue $\lambda_0 > 0$. Then there are $\mathcal{O}(\varepsilon^{3/2-d})$ values of the indices $(j, k) \in \mathbb{Z}_+^2$ such that (4.26) holds. Moreover, for these values of (j, k) the pearling eigenvalues of $\mathbb{L}$ satisfy*

$$\Lambda_p(j, k) = \varepsilon\left[\delta_0^2(j, k) + \frac{\int_{\mathbb{R}}[\eta_d W''(u_0) - v_0 W'''(u_0)]\psi_0^2 dr}{\|\psi_0\|_2^2}\right] + \mathcal{O}(\varepsilon\sqrt{\varepsilon}). \tag{4.30}$$

In particular α-single curvature bilayer interfaces are stable with respect to the pearling instability iff

$$\int_{\mathbb{R}}[v_0 W'''(u_0) - \eta_d W''(u_0)]\psi_0^2\, dr < 0, \tag{4.31}$$

or equivalently, recalling M_0 from (3.17), if and only if

$$(\eta_1 - \eta_2)\lambda_0\|\psi_0\|_2^2 - (\eta_1 + \eta_2)\frac{\|\dot{u}_0\|_2^2}{2M_0}S < 0. \tag{4.32}$$

Proof. When enumerated in order and according to multiplicity, the eigenvalues $\{\chi_n\}_{n=0}^\infty$ of the Laplace-Beltrami operator, Δ_s, satisfy the Weyl asymptotics

$$\chi_n \sim n^{2/(d-1)},$$

see [1]. Since $\chi_n = \beta(0, j, k) = \beta_0(j, k)$ for an ordered enumeration $n = n(j, k)$, the spacing between the sequential values of $\varepsilon^2\beta_0(j, k)$ near λ_0 scales like ε^{d-1}, and hence the values of $\delta_0 = \delta_0(j, k)$, see (4.26), for $(j, k) \in \mathcal{I}_p$, see (4.21), scale like $\varepsilon^{d-3/2}$. In particular $\delta_0^2(j, k)$ can be made as small as $\varepsilon^{2d-3} \ll 1$, for appropriate choices of (j, k). However there are $O(\varepsilon^{3/2-d}) \gg 1$ values of (j, k) for which $\delta_0(j, k) = O(1)$. Since δ_0 can

be made asymptotically small the pearling condition (4.31) follows from the eigenvalue asymptotics (4.30). It remains to derive the expression (4.32).

It follows from (3.14), (3.12), and the definition of ϕ_1 that v_0 can be decomposed as

$$v_0 = \gamma_1 \phi_1 - \frac{1}{2} r \eta_d \dot{u}_0, \tag{4.33}$$

so that the condition (4.31) is equivalent to,

$$\gamma_1 \int_{\mathbb{R}} \phi_1 W'''(u_0) \psi_0^2 \, dr - \frac{1}{2} \eta_d \int_{\mathbb{R}} \left[r W'''(u_0) \dot{u}_0 + 2 W''(u_0) \right] \psi_0^2 \, dr < 0. \tag{4.34}$$

Labeling the second integral in the expression above by I_2, integrating by parts, and using the eigenvalue problem for ψ_0 we obtain the expression,

$$
\begin{aligned}
I_2 &= \int_{\mathbb{R}} \left[(r\psi_0^2) \partial_r (W''(u_0)) + 2 W''(u_0) \psi_0^2 \right] dr \\
&= \int_{\mathbb{R}} (\psi_0 - 2r\dot{\psi}_0) W''(u_0) \psi_0 \, dr = \int_{\mathbb{R}} (\psi_0 - 2r\dot{\psi}_0)(\ddot{\psi}_0 - \lambda_0 \psi_0) \, dr \\
&= \int_{\mathbb{R}} \left[\partial_r (\psi_0 \dot{\psi}_0 - r\dot{\psi}_0^2 + r\lambda_0 \psi_0^2) - 2\lambda_0 \psi_0^2 \right] dr = -2\lambda_0 \|\psi_0\|_2^2.
\end{aligned}
$$

Expressing γ_1 in terms of η_1 and η_2 via (3.18), we derive (4.32).

4.4. The meander eigenmodes. The meander eigenvalues can be characterized in terms of the spectrum of $\mathbb{L}_{jk}$ for $(j,k) \in \mathcal{I}_m$, however their analysis is considerably more subtle, requiring a detailed understanding of the relation between the spectral stability problem and the derivative of the existence problem. The bilayer profile u_h solves the fourth-order system (3.1), which can also be expressed as

$$\left[\partial_r^2 - W''(u_h) + \varepsilon(\kappa \partial_r + \eta_1) \right] \circ \left[\ddot{u}_h - W'(u_h) + \varepsilon \kappa \dot{u}_h \right] + \varepsilon \eta_d W'(u_h) = \varepsilon \gamma.$$

As $\kappa = \kappa(r)$ is inhomogeneous, the problem is not translationally invariant in r. Indeed, acting ∂_r on this expression yields the relation

$$\mathbb{L}_{0,0} \, \dot{u}_h = -\varepsilon \left[\left((\partial_r^2 - W''(u_h)) + \varepsilon(\kappa \partial_r + \eta_1) \right) \circ (\dot{\kappa} \dot{u}_h) + \dot{\kappa} \partial_r (\ddot{u}_h - W'(u_h) + \varepsilon \kappa \dot{u}_h) \right], \tag{4.35}$$

where $\mathbb{L}_{0,0}$ is $\mathbb{L}_{j,k}$ from (4.15) with $j = k = 0$ for which $\beta(r; 0, 0) \equiv 0$. This result has the natural interpretation: the system (3.1) is translationally invariant in Cartesian coordinates, with the translational eigenfunctions corresponding to the modes $(j,k) \in \{(0,1), \ldots, (0,\alpha)\}$. The key observation, derived from (2.8) and (4.13), is that

$$\beta(r; 0, k) = -\frac{\dot{\kappa}}{\varepsilon},$$

for $k = 1, \ldots, \alpha$, from which we deduce that (4.35) is equivalent to

$$\mathbb{L}_{0,k} \, \dot{u}_h = 0, \tag{4.36}$$

also for $k = 1, \ldots, \alpha$. The relation (4.35) provides quantitative information about the meander eigenvalues and eigenfunctions $\Psi_m(x) = \psi_m(r) \mathcal{T}_j(\tau) \Theta_k(\theta)$, corresponding to potential long-wavelength shape instabilities. The eigenvalue and radial component of the eigenfunction admit the expansions

$$
\begin{aligned}
\Lambda_m(j,k) &= \varepsilon \Lambda_{1,m} + \varepsilon^2 \Lambda_{2,m} + \varepsilon^3 \Lambda_{3,m} + \varepsilon^4 \Lambda_{4,m} + \mathcal{O}(\varepsilon^5), \\
\psi_m(r; j, k) &= \dot{u}_0 + \varepsilon \psi_{1,m} + \varepsilon^2 \psi_{2,m} + \varepsilon^3 \psi_{3,m} + \varepsilon^4 \psi_{4,m} + \mathcal{O}(\varepsilon^5).
\end{aligned} \tag{4.37}
$$

From the expansions (3.23) and (3.24), and the relation (2.8), the equality (4.35) reduces to,

$$\mathbb{L}_{0,0} \, \dot{u}_h = \varepsilon^3 \frac{\alpha}{R_0^2} \left[2\dot{v}_0 + \frac{2(\alpha - 2)}{R_0} W'(u_0) + \eta_1 \dot{u}_0 \right] + \mathcal{O}(\varepsilon^4). \tag{4.38}$$

For the meander instability, we may restrict our attention to values of (j,k) for which $\beta(r; j, k) = \mathcal{O}(1)$ away from the boundary. Since β appears with a pre-factor ε^2, it follows that $\mathbb{L}_{0,0} = \mathbb{L}_{0,1} + \mathcal{O}(\varepsilon^2)$. Indeed, substitution of the expansions (4.37) into (4.15) shows that $\mathbb{L}_{0,1} \psi_m = \mathbb{L}_{0,0} \psi_m + \mathcal{O}(\varepsilon^3)$; moreover, from (4.38) we see that

$\mathbb{L}_{0,0}\dot{u}_h = \mathcal{O}(\varepsilon^3)$, and we deduce that Λ_m is at most $\mathcal{O}(\varepsilon^3)$ and the higher order terms $\dot{u}_1$ and $\dot{u}_2$ in the expansion of $\dot{u}_h$, see (3.23), appear in the higher order approximations of ψ_m.

LEMMA 4.4. *Let (j,k) be such that $\beta(r;j,k) = \mathcal{O}(1)$, then the associated meander eigenvalue $\Lambda_m(j,k) = O(\varepsilon^4)$ with eigenfunction ψ_m satisfying*

$$\psi_{0,m} = \dot{u}_0, \psi_{1,m} = \dot{u}_1, \psi_{2,m} = \dot{u}_2, \tag{4.39}$$

where u_j, $j = 0, 1, ..$, are defined in (3.23). Moreover,

$$\psi_{3,m} = \dot{u}_3 + \tilde{\psi}_3 = \dot{u}_3 + \alpha_{3,o}\tilde{\psi}_{3,o} + \alpha_{3,e}\tilde{\psi}_{3,e} \tag{4.40}$$

with,

$$\tilde{\psi}_{3,o} = -\tilde{u}_{2,o}, \tag{4.41}$$

where $\tilde{u}_{2,o}$ is defined in (3.25), and $\tilde{w}_{3,e}$ is the even solution of

$$\mathcal{L}\tilde{\psi}_{3,e} = r\dot{u}_0. \tag{4.42}$$

In addition, the coefficients follow the expansion (4.16), of β,

$$\alpha_{3,o} = \left(\beta_0 - \frac{\alpha}{R_0^2}\right), \ \alpha_{3,e} = \frac{1}{R_0}\left[\alpha\left(\beta_0 - \frac{\alpha}{R_0^2}\right) - 2\left(\beta_1 - \frac{\alpha}{R_0^2}\right)\right]. \tag{4.43}$$

REMARK 4.5. *In the case $(j,k) \in \{(0,1), \ldots, (0,\alpha)\}$, for which $\beta(r;j,k) = \frac{\alpha}{(R_0+\varepsilon r)^2}$, then $\psi_{3,m} = \dot{u}_3$, which is compatible with (4.36). This observation plays a central role in the proof of Lemma 4.6.*

Proof. We expand the eigenvalue problem for $\mathbb{L}_{jk}$, using the expansions (4.37), (3.23), and (4.15) in conjunction with (4.38). At $\mathcal{O}(\varepsilon)$ we obtain

$$\mathcal{L}^2\psi_{1,m} + \mathcal{R}_1 = \Lambda_{1,m}\dot{u}_0, \tag{4.44}$$

where we used (3.24), (3.33) with $\phi = \dot{u}_0$, and have introduced the residual

$$\mathcal{R}_1 := -\mathcal{L}\left[\dot{u}_0 u_1 W'''(u_0)\right] + \left[\eta_d W''(u_0) - v_0 W'''(u_0)\right]\dot{u}_0. \tag{4.45}$$

However, expanding (4.38) we find at the $\mathcal{O}(\varepsilon)$ order

$$\mathcal{L}^2\dot{u}_1 + \mathcal{R}_1 = 0, \tag{4.46}$$

which implies that $\langle\mathcal{R}_1, \dot{u}_0\rangle = 0$, and moreover $\Lambda_{1,m}\|\dot{u}_0\|_2^2 = \langle\mathcal{R}_1, \dot{u}_0\rangle = 0$, and hence $w_{1,m} = \dot{u}_1$. Similarly, at the $\mathcal{O}(\varepsilon^2)$-level we obtain

$$\begin{aligned}\mathcal{L}^2\psi_{2,m} &+ \mathcal{R}_2 &= \Lambda_{2,m}\dot{u}_0, \\ \mathcal{L}^2\dot{u}_2 &+ \mathcal{R}_2 &= 0,\end{aligned} \tag{4.47}$$

where we refrain from giving the particular expression for $\mathcal{R}_2$ since this is not relevant for the analysis. It *is* relevant that exactly the same expression $\mathcal{R}_2$ appears in both lines of (4.47). A priori one may expect terms from β to appear in the $\mathcal{O}(\varepsilon^2)$-level expansion of (4.15), terms that will not appear in the expansion of (4.38). However, since $\psi_m = \dot{u}_0$ at leading order, these terms do not appear. As at the $\mathcal{O}(\varepsilon)$ level, we deduce that $\Lambda_{2,m}\|\dot{u}_0\|_2^2 = \langle\mathcal{R}_2, \dot{u}_0\rangle = 0$, and hence $\psi_{2,m} = \dot{u}_2$.

At the $\mathcal{O}(\varepsilon^3)$-level, the expansion for the eigenvalue problem of (4.15) and for (4.38) differ non-trivially due to the expansion, (4.16), of β. We obtain

$$\begin{aligned}\mathcal{L}^2\psi_{3,m} &+ \mathcal{R}_{3,0} + \beta_0\mathcal{R}_{3,\beta_0} + \beta_1\mathcal{R}_{3,\beta_1} &= \Lambda_{3,m}\dot{u}_0, \\ \mathcal{L}^2\dot{u}_3 &+ \mathcal{R}_{3,0} &= \frac{\alpha}{R_0^2}\left[2\dot{v}_0 + \frac{2(\alpha-2)}{R_0}\ddot{u}_0 + \eta_1\dot{u}_0\right].\end{aligned} \tag{4.48}$$

where we have collected the terms with a β_0 prefactor,

$$\mathcal{R}_{3,\beta_0} := -2\dot{v}_0 - \frac{2\alpha}{R_0}\ddot{u}_0 - \eta_1\dot{u}_0, \tag{4.49}$$

and those with a β_1 prefactor,

$$\mathcal{R}_{3,\beta_1} := \frac{4}{R_0}\ddot{u}_0. \tag{4.50}$$

As before, the expression for $\mathcal{R}_{3,0}$ is not relevant to the analysis and is omitted. Using the existence condition (3.13) we deduce from the second line of (4.48) that

$$\langle \mathcal{R}_{3,0}, \dot{u}_0 \rangle = \frac{\alpha}{R_0^2}\left\langle \frac{2(\alpha-2)}{R_0}\ddot{u}_0, \dot{u}_0 \right\rangle + \langle 2\dot{v}_0 + \eta_1\dot{u}_0, \dot{u}_0 \rangle = 0,$$

Hence from the first line of (4.48), we infer that,

$$\Lambda_{3,m}\|\dot{u}_0\|_2^2 = \beta_0\langle \mathcal{R}_{3,\beta_0}, \dot{u}_0 \rangle + \beta_1\langle \mathcal{R}_{3,\beta_1}, \dot{u}_0 \rangle = -\beta_0\left[\langle 2\dot{v}_0 + \eta_1\dot{u}_0, \dot{u}_0 \rangle\right] - \frac{2\left(\alpha\beta_0 - 2\beta_1\right)}{R_0}\langle \ddot{u}_0, \dot{u}_0 \rangle = 0,$$

where again we applied (3.13). While $\Lambda_{3,m} = 0$, we observe from (4.48)-(4.50) that,

$$\begin{aligned}
\mathcal{L}^2(\psi_{3,m} - \dot{u}_3) &= \left(\beta_0 - \frac{\alpha}{R_0^2}\right)\left[2\dot{v}_0 + \frac{2\alpha}{R_0}\ddot{u}_0 + \eta_1\dot{u}_0\right] - \frac{4}{R_0}\left(\beta_1 - \frac{\alpha}{R_0^2}\right)\ddot{u}_0 \\
&= \left(\beta_0 - \frac{\alpha}{R_0^2}\right)[2\dot{v}_0 + \eta_1\dot{u}_0] + \frac{1}{R_0}\left[\alpha\left(\beta_0 - \frac{\alpha}{R_0^2}\right) - 2\left(\beta_1 - \frac{\alpha}{R_0^2}\right)\right](2\ddot{u}_0).
\end{aligned}$$

The decomposition (4.40) of $\psi_{3,m}$ with pre-factors (4.43) thus follows naturally. Moreover, (4.41) follows from (3.26), and (4.42) follows from (3.14). $\qquad\square$

The meander eigenvalues are resolved at $\mathcal{O}(\varepsilon^4)$:

LEMMA 4.6. *Under the assumptions of Lemma 4.4 the meander eigenvalue* $\Lambda_m(j,k)$ *of* $\mathbb{L}_{jk}$, *satisfies*

$$\Lambda_m = \varepsilon^4\left[\left(\beta_0 - \frac{\alpha}{R_0^2}\right)\left(\beta_0 + \frac{\alpha^2}{R_0^2}\right) - \left(\beta_1 - \frac{\alpha}{R_0^2}\right)\left(\frac{2\alpha}{R_0^2}\right)\right] + \mathcal{O}\left(\varepsilon^5\right). \tag{4.51}$$

Proof. Using the notation of Lemma 4.4, the eigenvalue problem for $\mathbb{L}_{jk}$, defined in (4.15), admits the expansion,

$$\mathcal{L}^2\psi_{4,m} + \mathcal{R}_{4,0} + \beta_0\mathcal{R}_{4,\beta_0} + \beta_1\mathcal{R}_{4,\beta_1} + \beta_2\mathcal{R}_{4,\beta_2} + \beta_0^2\mathcal{R}_{4,\beta_0^2}(u_i) = -\Lambda_{4,m}\dot{u}_0. \tag{4.52}$$

Since $\psi_{3,m} \not\equiv \dot{u}_3$, the relation between the $\mathcal{O}(\varepsilon^4)$-expansions of (4.15) and of (4.38) are less transparent than the expansions in the proof of Lemma 4.4. It is straightforward to check that in (4.52) only $\mathcal{R}_{4,0}$ depends on $\psi_{3,m}$ and that it depends linearly upon $\psi_{3,m}$. By (4.40) we therefore decompose $\mathcal{R}_{4,0}$ into

$$\mathcal{R}_{4,0} = \mathcal{R}_{4,0,0} + \tilde{\mathcal{R}}_1\tilde{\psi}_3 \tag{4.53}$$

where $\tilde{\mathcal{R}}_1$ a linear operator – see (4.59) below – and $\mathcal{R}_{4,0,0}$, also appears in the $\mathcal{O}(\varepsilon^4)$-expansion of (4.38). By (4.52), (4.53) and (4.40) it is natural to decompose $\Lambda_{4,m}$ into,

$$\Lambda_{4,m} = \Lambda_{4,0,0} + \alpha_{3,o}\Lambda_{4,3,o} + \alpha_{3,e}\Lambda_{4,3,e} + \beta_0\Lambda_{4,\beta_0} + \beta_1\Lambda_{4,\beta_1} + \beta_2\Lambda_{4,\beta_2} + \beta_0^2\Lambda_{4,\beta_0^2}, \tag{4.54}$$

where the coefficients of $\Lambda_{4,m}$ satisfy

$$\begin{aligned}
\Lambda_{4,0,0} &= \frac{\langle \mathcal{R}_{4,0,0}, \dot{u}_0 \rangle}{\|\dot{u}_0\|_2^2}, & \Lambda_{4,3,o} &= \frac{\langle \tilde{\mathcal{R}}_1\tilde{\psi}_{3,o}, \dot{u}_0 \rangle}{\|\dot{u}_0\|_2^2}, & \Lambda_{4,3,e} &= \frac{\langle \tilde{\mathcal{R}}_1\tilde{\psi}_{3,e}, \dot{u}_0 \rangle}{\|\dot{u}_0\|_2^2}, \\
\Lambda_{4,\beta_0} &= \frac{\langle \mathcal{R}_{4,\beta_0}, \dot{u}_0 \rangle}{\|\dot{u}_0\|_2^2}, & \Lambda_{4,\beta_1} &= \frac{\langle \mathcal{R}_{4,\beta_1}, \dot{u}_0 \rangle}{\|\dot{u}_0\|_2^2}, & \Lambda_{4,\beta_2} &= \frac{\langle \mathcal{R}_{4,\beta_2}, \dot{u}_0 \rangle}{\|\dot{u}_0\|_2^2}, \\
\Lambda_{4,\beta_0^2} &= \frac{\langle \mathcal{R}_{4,\beta_0^2}, \dot{u}_0 \rangle}{\|\dot{u}_0\|_2^2}. &&&&
\end{aligned} \tag{4.55}$$

It readily follows from the expansion of $\mathbb{L}_{0,1}$ that $\mathcal{R}_{4,\beta_0^2}(\dot{u}_0) = \dot{u}_0$, so that

$$\Lambda_{4,\beta_0^2} = 1. \tag{4.56}$$

Straightforward manipulations yield that

$$\langle \mathcal{R}_{4,\beta_1}, \dot{u}_0 \rangle = \frac{2\alpha}{R_0^2} \left[\langle \partial_r(r\dot{u}_0), \dot{u}_0 \rangle + \langle r\ddot{u}_0, \dot{u}_0 \rangle \right], \ \langle \mathcal{R}_{4,\beta_2}, \dot{u}_0 \rangle = -\frac{6}{R_0^2} \langle \dot{u}_0 + 2r\ddot{u}_0, \dot{u}_0 \rangle,$$

so that we find by (3.33) with $\phi = \dot{u}_0$ and the identity $\langle r\ddot{u}_0, \dot{u}_0 \rangle = -\|\dot{u}_0\|_2^2/2$, that

$$\Lambda_{4,\beta_1} = \Lambda_{4,\beta_2} = 0. \tag{4.57}$$

Moreover,

$$\langle \mathcal{R}_{4,\beta_0}, \dot{u}_0 \rangle = \frac{2\alpha}{R_0^2} \int_{\mathbb{R}} r\dot{u}_0\ddot{u}_0 \, dr - \eta_1 \int_{\mathbb{R}} \dot{u}_0 \dot{u}_1 \, dr + \int_{\mathbb{R}} \left[2(\dot{u}_0 u_1 \dot{u}_1 + \dot{u}_0^2 u_2)W'''(u_0) + \dot{u}_0^2 u_1^2 W''''(u_0) \right] dr,$$

so that by (3.33) with $\phi = \dot{u}_0$ and the higher order existence condition (3.35) of Lemma 3.5,

$$\Lambda_{4,\beta_0} = -\frac{\alpha}{R_0^2} + \frac{\langle 2\dot{v}_0 + \eta_1\dot{u}_0, \dot{u}_1 \rangle}{\|\dot{u}_0\|_2^2}. \tag{4.58}$$

Finally, from the $\mathcal{O}(\varepsilon^4)$ expansion of $\mathbb{L}_{jk}$, we deduce that the action of the operator $\tilde{\mathcal{R}}_1$ on a function $\tilde{\psi}$ takes the form,

$$\tilde{\mathcal{R}}_1\tilde{\psi} = \frac{2\alpha}{R_0}\partial_r\left[\mathcal{L}\tilde{\psi}\right] + \left[\eta_1 - u_1 W'''(u_0)\right]\mathcal{L}\tilde{\psi} - \mathcal{L}\left[u_1 W'''(u_0)\tilde{\psi}\right] + \left[\eta_d W''(u_0) - v_0 W'''(u_0)\right]\tilde{\psi}. \tag{4.59}$$

This expression coincides with (4.45) if $\tilde{\psi}$ is replaced by $\dot{u}_0$. This is a natural consequence of the structure of the expansion procedure, and motivates the subscript 1 in the notation introduced in (4.53). Using (4.41), (4.42), (3.26), (3.27), (3.33) with various ϕ's, and the fact that $\tilde{\psi}_{3,o}$ and $\tilde{\psi}_{3,e}$, are respectively odd and even as functions of r, we deduce,

$$\begin{aligned}
\langle \tilde{\mathcal{R}}_1\tilde{\psi}_{3,o}, \dot{u}_0 \rangle &= \langle [\eta_1 - u_1 W'''(u_0)]\mathcal{L}\tilde{\psi}_{3,o}, \dot{u}_0 \rangle + \langle [\eta_d W''(u_0) - v_0 W'''(u_0)]\tilde{\psi}_{3,o}, \dot{u}_0 \rangle \\
&= \langle u_1 W'''(u_0)\tilde{v}_{1,o}, \dot{u}_0 \rangle - \eta_d\langle W''(u_0)\tilde{u}_{2,o}, \dot{u}_0 \rangle + \langle v_0 W'''(u_0)\tilde{u}_{2,o}, \dot{u}_0 \rangle \\
&= -\left[\langle \tilde{v}_{1,o}, \dot{v}_0 \rangle + \langle 2v_0 + \eta_1\dot{u}_0, \dot{u}_0 \rangle \right] + \eta_d\langle \dot{\tilde{u}}_{2,o}, \ddot{u}_0 \rangle + \left[\langle \tilde{v}_{1,o}, \dot{v}_0 \rangle - \eta_d\langle \dot{\tilde{u}}_{2,o}, \ddot{u}_0 \rangle \right] \\
&= -\langle 2v_0 + \eta_1\dot{u}_0, \dot{u}_0 \rangle,
\end{aligned}$$

and,

$$\langle \tilde{\mathcal{R}}_1\tilde{\psi}_{3,e}, \dot{u}_0 \rangle = \frac{2\alpha}{R_0}\langle \partial_r\left[\mathcal{L}\tilde{w}_{3,e}\right], \dot{u}_0 \rangle = \frac{\alpha}{R_0}\|\dot{u}_0\|_2^2.$$

It follows that

$$\Lambda_{4,3,o} = -\frac{\langle 2\dot{v}_0 + \eta_1\dot{u}_0, \dot{u}_1 \rangle}{\|\dot{u}_0\|_2^2}, \ \Lambda_{4,3,e} = \frac{\alpha}{R_0} \tag{4.60}$$

By combining the expressions (4.54), (4.56), (4.57), (4.58), and (4.60), we obtain the relation

$$\Lambda_{4,m} = \Lambda_{4,0,0} - \alpha_{3,o}\frac{\langle 2\dot{v}_0 + \eta_1\dot{u}_0, \dot{u}_1 \rangle}{\|\dot{u}_0\|_2^2} + \alpha_{3,e}\frac{\alpha}{R_0} - \beta_0\left(\frac{\alpha}{R_0^2} - \frac{\langle 2\dot{v}_0 + \eta_1\dot{u}_0, \dot{u}_1 \rangle}{\|\dot{u}_0\|_2^2} \right) + \beta_0^2. \tag{4.61}$$

A key step is to use the translational symmetries, in the guise of (4.36), to deduce that $\Lambda_{4,m} = 0$ when $\beta_0 = \beta_1 = \frac{\alpha}{R_0^2}$. In this manner we derive the value of $\Lambda_{4,0,0}$ without determining $\langle \mathcal{R}_{4,0,0}, \dot{u}_0 \rangle$ directly. Indeed, substituting these values into (4.61), and using (4.43) we determine that

$$\Lambda_{4,0,0} = -\frac{\alpha}{R_0^2}\frac{\langle 2\dot{v}_0 + \eta_1\dot{u}_0, \dot{u}_1 \rangle}{\|\dot{u}_0\|_2^2}. \tag{4.62}$$

Substitution of (4.43) and (4.62) into (4.61) and simplifying the expressions for v_0 and u_1 yields (4.51). $\qquad\square$

COROLLARY 4.7. *Fix $d \geq 2$, and let $\mathbb{L}$, given by (4.2), be the second variational derivative of $\mathcal{F}$ at a co-dimension one α-single curvature bilayer morphology U_h. If the pearling stability condition (4.32) holds*

then $\dim \ker(\mathbb{L}) = \alpha$ *with the kernel spanned by the* α *translational eigenfunctions. In addition, if* $\alpha = 1$ *then* $n(\mathbb{L}) = 0$, *if* $\alpha = 2$ *or* $\alpha = d - 1$, *then* $n(\mathbb{L}) \leq 1$ *with the potential negative space spanned by the purely radial meander eigenfunction* $\Psi_m(r; 0, 0)$, *while if* $\alpha \in \mathbb{Z}_+ \cap [3, d-2]$, *which requires* $d \geq 5$, *then*

$$n(\mathbb{L}) = \# \left\{ (n_1, \ldots, n_K) \in \mathbb{Z}_+^K \, \middle| \, \pi^2 \sum_{j=1}^{K} \left(\frac{n_j}{L_j} \right)^2 \leq \frac{\alpha}{2R_0^2} \left(1 - \alpha + \sqrt{\alpha^2 + 2\alpha - 7} \right) \right\}. \tag{4.63}$$

in particular $n(\mathbb{L})$ *grows with decreasing* R_0 *and increasing size of* Ω. *In this latter case the negative space consists of eigenfunctions with variation only in the flat directions. In each case there exists* $C > 0$, *independent of* ε *such that the positive meander eigenvalues of* $\mathbb{L}$ *satisfy* $\Lambda_m(j, k) > C\varepsilon^4$.

Proof. The eigenvalues $\{\mu_j\}_{j=0}^{\infty}$ of Δ_τ satisfy $\mu_0 = 0$ while $\mu_j \geq \mu_1$ for $j \geq 1$. In particular the lower bound on μ_1 depends only upon α, d, and the size of Ω. On the other hand the eigenvalues $\{\nu_k\}_{k=0}^{\infty}$ of Δ_θ satisfy $\nu_0 = 0$, $\nu_1 = \ldots = \nu_\alpha = \alpha$, and $\nu_k > \alpha$ for $k \geq \alpha + 2$. Inserting the terms from (4.16) into (4.51) we find that

$$\Lambda_m(j, k) = \varepsilon^4 \left[\mu_j^2 + \frac{2\nu_k + \alpha^2 - \alpha}{R_0^2} \mu_j + \frac{\nu_k - \alpha}{R_0^4} (\nu_k + \alpha^2 - 2\alpha) \right] + \mathcal{O}(\varepsilon^5). \tag{4.64}$$

If $\nu_k > \alpha$, then Λ_m must be strictly positive. If $\nu_k = \alpha$, then Λ_m is either strictly positive, or zero at leading order when $\mu_j = 0$. This latter case corresponds precisely to the translation eigenvalues in the kernel of $\mathbb{L}$, up to exponentially small terms. If $\nu_k = 0$, then Λ_m takes negative values if

$$0 \leq \mu_j R_0^2 < \frac{\alpha}{2} \left(1 - \alpha + \sqrt{\alpha^2 + 2\alpha - 7} \right), \tag{4.65}$$

and is $O(\varepsilon^5)$, and of indeterminate sign, in the case of equality in the second relation. In particular this degenerate case occurs if $\alpha = 2$ and $\mu_j = 0$. If $\alpha = d - 1$, in which case there are no straight directions, then μ_j is replaced with 0 and the eigenvalue associated to $\nu_0 = 0$ is negative. However there are a potential abundance of negative eigenvalues if $\alpha \in \mathbb{Z} \cap [3, d - 2]$ and R_0 is sufficiently small, as quantified in (4.63). $\qquad \square$

4.5. The spectrum of $\mathbb{L}_0$ restricted to $\mathcal{Z}_{0,0}$. As explained in section 4.2, we can finalize the spectral analysis by studying the spectrum of $\mathbb{L}_0$ as it acts on the invariant space $\mathcal{Z}_{0,0}$. In light of Corollary 4.7 and Lemma 4.2, we can have $n(\mathbb{L}_0) = 0$ only if there is no pearling instability and if $n(\mathbb{L}) \leq 1$ which occurs for $\alpha = 1, 2$, and $d - 1$. In particular, in the cases when $n(\mathbb{L}) = 1$, the negative space, corresponding to the red-box eigenvalue in Figure 4.2, is a subset of $\mathcal{Z}_{0,0}$ and hence amenable to stabilization by the mass constraint.

LEMMA 4.8. *The space* $\mathcal{Z}_{0,0}$ *is invariant under* $\mathbb{L}$ *and* Π_0, *moreover there exists a* $\sigma_{0,0} > 0$, *independent of* ε *such that the operator,* $\mathbb{L}_{0,0}$, *obtained by restricting* $\mathbb{L}$ *to* $\mathcal{Z}_{0,0}$, *satisfies*

$$n(\Pi_0 \mathbb{L}_{0,0} - \sigma_{0,0} \varepsilon^3) = 0, \tag{4.66}$$

in particular, $\sigma(\Pi_0 \mathbb{L}_{0,0}) \subset [\sigma_{0,0} \varepsilon^3, \infty)$.

Together with Lemma 4.3 and Corollary 4.7, Lemma 4.8 completes the proof of Theorem 1.2 – see section 4.2.

Proof. From (4.51) the spectra of $\mathbb{L}_{0,0}$ consists of one small eigenvalue, $\Lambda_m(0, 0) = O(\varepsilon^4)$, with the rest of its spectra contained inside of $[\overline{\sigma}, \infty)$, see Figure 4.2 and (4.18). In particular $n(\mathbb{L}_{0,0} - \sigma_{0,0} \varepsilon^3) = 1$ for all $0 < \sigma_{0,0} = \mathcal{O}(1)$, and applying Lemma 4.2 to $\mathbb{L}_{0,0} - \sigma_{0,0} \varepsilon^3$ we deduce that the smallest eigenvalue of $\Pi_0 \mathbb{L}_{0,0}$ equals the smallest value of σ_0 which makes

$$g(\sigma_0) := \left\langle (\mathbb{L}_{0,0} - \sigma_{0,0} \varepsilon^3)^{-1} 1, 1 \right\rangle_{\Omega}, \tag{4.67}$$

zero. To estimate $\sigma_{0,0}$ we decompose the function 1 as

$$1 = c_m \Psi_m(0, 0) + \Psi^{\perp}, \tag{4.68}$$

where $\Psi^{\perp} \in \mathcal{Z}_{0,0}$ is $L^2(\Omega)$ orthogonal to the eigenfunction Ψ_m, which satisfies the expansions (4.39). Since the functions in the decomposition are orthogonal we have

$$|\Omega| = \|1\|_{L_\Omega^2}^2 = c_m^2 \|\Psi_m\|_{L_\Omega^2}^2 + + \|\Psi^{\perp}\|_{L_\Omega^2}^2,$$

in particular each term is uniformly bounded. Moreover, using (2.10) we observe that

$$c_m = \frac{\langle 1, \Psi_m \rangle_\Omega}{\|\Psi_m\|_{L^2}^2} = \varepsilon \frac{|\Gamma|}{\|\Psi_m\|_{L_\Omega^2}^2} \int_{\mathbb{R}} (\dot{u}_0 + \varepsilon \dot{u}_1 + O(\varepsilon^2)) (R_0 + \varepsilon r)^\alpha dr = -\varepsilon^2 \frac{\alpha R_0^{\alpha-1} M_0 |\Gamma|}{\|\Psi_m\|_{L^2}^2} + O(\varepsilon^3) \qquad (4.69)$$

where M_0 is defined in (3.17). Using the orthogonality of the decomposition (4.68) we have

$$g(\sigma_0) = \frac{c_m^2 \|\Psi_m\|_{L_\Omega^2}^2}{\Lambda_m - \sigma_{0,0}\varepsilon^3} + + \left\langle (\mathbb{L}_{0,0} - \sigma_{0,0}\varepsilon^3)^{-1} \Psi^\perp, \Psi^\perp \right\rangle_\Omega . \qquad (4.70)$$

However, $(\mathbb{L}_{0,0} - \sigma_{0,0}\varepsilon^3)^{-1}$ is uniformly bounded on $\Psi^\perp$, hence the last term is $O(1)$, in both ε and $\sigma_{0,0}$. Moreover

$$\|\Psi_m\|_{L_\Omega^2}^2 = \varepsilon |\Gamma| \|\dot{u}_0\|_2^2 + \mathcal{O}(\varepsilon^2),$$

and from (4.64) evaluated at $(j, k) = (0, 0)$ we deduce

$$g(\sigma_0) = -\frac{\alpha^2 R_0^{2+2\alpha} M_0^2 |\Gamma|}{\sigma_{0,0} + \varepsilon\alpha^2(\alpha - 2))\|\dot{u}_0\|_2^2} + \mathcal{O}(1). \qquad (4.71)$$

Taking $\sigma_{0,0}$ sufficiently small, independent of ε, we find, for ε sufficiently small (which may depend upon $\sigma_{0,0}$), that $n(g(\sigma_0)) = n(\mathbb{L}_{0,0} - \sigma_{0,0}\varepsilon^3)$ and hence (4.66) follows from Lemma 4.2. □

4.6. The flat interface. The case of a flat interface, $\alpha = 0$, requires two adjustments to the stability analysis. First, as there are no curved directions, we replace ν_k with 0. Second, the existence condition (3.18) for u_h is not required, and as expressed in Corollary 3.2 we have a family of homoclinic orbits, u_h, parameterized by γ_1.

COROLLARY 4.9. *Fix $d \geq 2$ and $\alpha = 0$. Let u_h be the homoclinic orbit, established in Corollary 3.2, parameterized by $\gamma_1 \in \mathbb{R}$. For ε small enough, the function U_h obtained by dressing Γ with u_h is linearly stable under the FCH evolution if and only if γ_1 satisfies the pearling*

$$\gamma_1 S + \lambda_0(\eta_1 - \eta_2)\|\psi_0\|_2^2 < 0, \qquad (4.72)$$

and the meander

$$\gamma_1 M_0 + \frac{1}{2}(\eta_1 + \eta_2)\|\dot{u}_0\|_2^2 < 0, \qquad (4.73)$$

stability conditions, where the shape factor S and the interfacial mass M_0, are defined in (4.28) and (3.17) respectively.

REMARK 4.10. *The role of the shape factor, S, in (4.72) and (4.32) is now transparent. Since γ_1 controls the perturbations to the back-ground state of solvent, the sign of the shape factor determines if pearling is induced by dehydration, that is lowering the background level of solvent, or by over-hydration, i.e., raising the background level of solvent above the equilibria level.*

Proof. The relation of (4.72) follows immediately from the derivation of (4.32) from (4.34) without the substitution (3.18) for γ_1. The $\alpha = 0$ counterpart of the meandering analysis by replacing ν_k with 0 in section 4.4 and especially in the proof of Lemma 4.4. The first significant changes appears at the $\mathcal{O}(\varepsilon^3)$-level, where both the β_1-term in the first equation of (4.48) and the right-hand side term of the second equation of (4.48) vanish (since $\alpha = \beta_1 = 0$). On the other hand,

$$\langle \mathcal{R}_{3,\beta_0}, \dot{u}_0 \rangle = -\langle 2\dot{v}_0 + \eta_1 \dot{u}_0, \dot{u}_0 \rangle \neq 0,$$

see (4.49), since the existence condition, see (3.13), need not hold for $\alpha = 0$. Hence, by (4.48) and (4.16) we have,

$$\Lambda_{3,m}(j) = -\beta_0 \frac{\langle \mathcal{R}_{3,\beta_0}, \dot{u}_0 \rangle}{\|\dot{u}_0\|_2^2} = -\mu_j \frac{\langle 2\dot{v}_0 + \eta_1 \dot{u}_0, \dot{u}_0 \rangle}{\|\dot{u}_0\|_2^2}.$$

Since the eigenvalue $\Lambda_{3,m}(0)=0$ corresponds to the translational symmetry, and $\mu_j > 0$ for $j \geq 1$, the flat interfaces possess positive meander eigenvalues iff $\langle 2\dot{v}_0 + \eta_1 \dot{u}_0, \dot{u}_0 \rangle < 0$. This condition is equivalent to (4.73) by (3.15) – compare also (4.73) to (3.18). Since the kernel of $\mathbb{L}$ is spanned by the massless translational eigenvalue, with negative eigenvalues coming from massless pearling modes or meander modes, the projection Π_0 has no impact on the negative index. □

4.7. Asymptotic form of the eigenfunctions. From Lemmas 4.3, 4.6, and 4.8 we know that, in all cases, the spectra $\sigma(\mathbb{L}_0)\backslash\{0\} \subset [\nu\varepsilon, \infty)$ for some $\nu \in \mathbb{R}$ independent of ε. If, in addition $\nu > 0$, then from Lemma 4.1 we deduce that $\sigma(-\mathcal{G}\mathbb{L})\backslash\{0\} \subset (-\infty, -\nu C_1\varepsilon]$, where $C_1 > 0$, defined in (4.3), is independent of ε. However if $\mathcal{G}$ is an unbounded operator, then these estimates are not asymptotically sharp, and in particular if $\nu < 0$ then $-\mathcal{G}\mathbb{L}$ may have large positive spectra. However the spectra of $-\mathcal{G}\mathbb{L}$ varies smoothly in the parameters η_1 and η_2 and during bifurcation which triggers instability, when spectra crosses zero to become positive, the spectra must be small. If in addition the spaces $\mathcal{Z}_{jk}$ are invariant under the gradient $\mathcal{G}$, as is the case if $\mathcal{G} = G(-\Delta)$ for $G : \mathbb{R}_+ \mapsto \mathbb{R}_+$ a smooth positive function, then the eigenfunctions of $-\mathcal{G}\mathbb{L}$ associated to its small eigenvalues are comprised, at leading order, of either the meander or the pearling eigenfuctions of $\mathbb{L}$.

PROPOSITION 4.11. *Assume that the spaces $\mathcal{Z}_{jk}$, defined in (4.14) are invariant under $\mathcal{G}$. Then for each $U > 0$ sufficiently small there exists $\nu > 0$ such that the eigenfunction $\Psi_\mathcal{G}$ associated to any eigenvalue $\Lambda_\mathcal{G} \in \sigma(-\mathcal{G}\mathbb{L})\backslash\{0\}\cap[-U, U]$ lies in $\mathcal{Z}_{jk}$, defined in (4.14), for some (j, k) from either $\mathcal{I}_m$ or $\mathcal{I}_p$, defined in (4.20) and (4.21), respectively. Moreover, in either the pearling or the meander case, the radial component $\psi_{\mathcal{G}(r),m/p}$ of the eigenfunction $\Psi_{\mathcal{G},m/p}(x; j, k) = \psi_{\mathcal{G},m/p}(r)\mathcal{T}_j(\tau)\Theta_k(\theta)$ admits the decomposition*

$$\psi_{\mathcal{G},m/p}(r; j, k) = \psi_{m/p}(r; j, k) + \psi^\perp_{m/p}(r; j, k), \tag{4.74}$$

where ψ_m or ψ_p are the radial components of the meander and pearling eigenmodes of $\mathbb{L}$, and $\psi^\perp_{m/p} \in L^2(\mathbb{R})$ is orthogonal to ψ_m or ψ_p, respectively, and satisfies

$$\|\psi^\perp_{m/p}\|_2 \leq \frac{|\Lambda_\mathcal{G}|}{\nu}\|\psi_{\mathcal{G},m/p}\|_2. \tag{4.75}$$

Proof. Since the operator $-\mathcal{G}\mathbb{L}$ leaves the disjoint spaces $\mathcal{Z}_{j,k}$ invariant, and since the spaces collectively span $L^2(\Omega)$, it follows that each distinct eigenspace of $-\mathcal{G}\mathbb{L}$ is contained entirely within one of the $\mathcal{Z}_{j,k}$. Let $\mathcal{G}_{jk}$ denote the restriction of $\mathcal{G}$ to $\mathcal{Z}_{jk}$. If $\lambda_\mathcal{G} \in \sigma(-\mathcal{G}_{jk}\mathbb{L}_{jk})$ is sufficiently small, as controlled by $U > 0$, then by a slight modification of Lemma 4.1, $\sigma(\mathbb{L}_{jk})$ also has a small eigenvalue. Since the sets $\mathcal{I}_m$ and $\mathcal{I}_p$ are disjoint, this is the only small eigenvalue of $\mathbb{L}_{jk}$ and either $(j, k) \in \mathcal{I}_m$ or $(j, k) \in \mathcal{I}_p$. Without loss of generality we consider the meander case, and perform the corresponding decomposition of the form (4.74). For $\Lambda_\mathcal{G} \neq 0$ the eigenfunction $\Psi_{\mathcal{G},m}$ has zero-mass and the associated eigenvalue problem can be written in the form

$$\Lambda_m\psi_m + \mathbb{L}_{jk}\psi^\perp_m = -\Lambda_\mathcal{G}\mathcal{G}^{-1}_{jk}\psi_{\mathcal{G},m}.$$

Taking the $L^2(\mathbb{R})$ norm and using the orthogonality of the components we obtain the equality

$$\Lambda^2_m\|\psi_m\|^2_2 + \|\mathbb{L}_{jk}\psi^\perp\|^2_2 = |\Lambda_\mathcal{G}|^2\|\mathcal{G}^{-1}_{j,k}\psi_\mathcal{G}\|^2_{L^2_\Omega}. \tag{4.76}$$

However, for $(j, k) \in \mathcal{I}_m$ the operator $\mathbb{L}_{jk}$ is uniformly coercive in the $\|\cdot\|_2$ norm on $(\text{span}\{\psi_m(j, k)\})^\perp$, with a bound, $\tilde{\nu} > 0$, which may be chosen independent of ε and (j, k), while $\mathcal{G}^{-1}_{j,k}$ is uniformly bounded by C^{-1}_1; defining $\nu = \tilde{\nu}C_1$ yields (4.75). □

5. Explicit class of potential wells and simulations.

5.1. An explicit class of potentials $W_p(u)$. The bifurcation of α-single curvature interfaces is explicitly influenced by the two functionalization parameters η_1 and η_2 which appear in the FCH gradient flow, (1.4). However the form of the double-well potential W plays a less transparent role in determining stability. Of particular interest is the sign of the shape factor, S, see (4.28), and whether it can be changed by variation in the well W. In this section we answer these questions for an explicit family of well shapes.

For $p > 2$ we define the potential $\tilde{W}_p(\tilde{u})$,

$$\tilde{W}_p(\tilde{u}) = \frac{1}{p - 2}\left(p\tilde{u}^2 - 2\tilde{u}^p\right). \tag{5.1}$$

The potential $\tilde{W}(\tilde{u})$ is not a double well potential, having only one minimum at $\tilde{u} = 0$, a maximum at $\tilde{u} = 1$, and a second zero, $\tilde{m}_p$, given by

$$\tilde{m}_p = \left(\frac{p}{2}\right)^{\frac{1}{p-2}} > 1, \tag{5.2}$$

where we note that

$$\lim_{p \downarrow 2} \tilde{m}_p = \sqrt{e}, \quad \lim_{p \to \infty} \tilde{m}_p = 1. \tag{5.3}$$

Our analysis depends upon the double well potential $W_p(u)$ solely through its values for $u \in [-1, m_0 + O(\varepsilon)]$, where m_0 is its second zero, thus we fix $\delta > 0$, independent of ε, and define

$$W_p(u) := \tilde{W}_p(u + 1) \quad \text{for} \quad u < \tilde{m}_p - 1 + \delta, \tag{5.4}$$

and extend W_p smoothly for $u \geq \tilde{m}_p - 1 + \delta$ so that it has a second well; in particular satisfying the assumptions below (1.1) with

$$\mu_- = \frac{2p}{p-2} > 0, \quad m = \tilde{m}_p - 1 = \left(\frac{p}{2}\right)^{\frac{1}{p-2}} - 1 > 0, \quad \mu_0 = -2p < 0. \tag{5.5}$$

The parameter μ_- controls the exponential decay rate of u_0, which becomes infinite as $p \downarrow 2$, but takes a finite, non-zero value as $p \to \infty$. The following results, established in the Appendix, relate the values of the key parameters to the integral

$$\mathcal{I}(q) := \int_0^1 \left(1 - y^2\right)^q \, dy, \tag{5.6}$$

which is decreasing in $q > 0$, taking values in $(0, 1)$, and is a scaled form of the (Euler) beta function $\mathcal{B}(x, y)$, see for instance [22], with $x = y = q + 1$,

$$\mathcal{I}(q) = 4^q \int_0^1 z^q (1 - z)^q \, dz = 4^q \, \mathcal{B}(q + 1, q + 1).$$

LEMMA 5.1. *Fix $p > 2$ and let $u_0 = u_0(r; p)$ be the homoclinic solution of (3.8) for $W = W_p$. Then the ground state eigenvalue and eigenfunction of the linearized operator $\mathcal{L}$, defined in (3.11), satisfy*

$$\lambda_0 = \frac{1}{2} p(p + 2) > 0, \qquad \psi_0 = (u_0 + 1)^{\frac{1}{2}p} > 0. \tag{5.7}$$

Moreover, recalling $\tilde{m}_p$, defined in (5.2), the following equalities hold

$$\|\dot{u}_0\|_2^2 = \|\psi_0\|_2^2 = \frac{2}{\sqrt{p-2}} \, \tilde{m}_p^{\frac{1}{2}(p+2)} \, \mathcal{I}\left(\frac{2}{p-2}\right), \tag{5.8}$$

while the unit mass M_0, the shape factor S, defined in (3.17) and (4.28), satisfy

$$M_0 = \frac{2}{\sqrt{p-2}} \, \tilde{m}_p^{\frac{1}{2}p} \, \mathcal{I}\left(\frac{1}{p-2}\right), \tag{5.9}$$

$$S = -\frac{2(p-1)}{\sqrt{p-2}} \, \tilde{m}_p^{\frac{1}{2}(3p-4)} \, \mathcal{I}\left(\frac{1}{p-2}\right). \tag{5.10}$$

The following remarkably transparent result is obtained by substitution of the expressions from Lemma 5.1 into (4.32).

COROLLARY 5.2. *Fix $d \geq 2$ and $\alpha \in \{1, \ldots, d-1\}$. For the class of potentials $W_p(u)$, defined in (5.4), the pearling stability condition (4.32) reduces to*

$$0 < \eta_1 < \frac{1}{3} \frac{p+5}{p+1} \eta_2. \tag{5.11}$$

For the flat case, $\alpha = 0$, the pearling and meander stability conditions (4.72) and (4.73) are satisfied for all γ_1 such that,

$$\tilde{m}_p \frac{\mathcal{I}\left(\frac{2}{p-2}\right)}{\mathcal{I}\left(\frac{1}{p-2}\right)} \left[\frac{p+2}{p-1} (\eta_1 - \eta_2)\right] < \gamma_1 < \tilde{m}_p \frac{\mathcal{I}\left(\frac{2}{p-2}\right)}{\mathcal{I}\left(\frac{1}{p-2}\right)} \left[-\frac{1}{2} (\eta_1 + \eta_2)\right]. \tag{5.12}$$

In particular the upper and lower bounds on γ_1 are no-overlapping precisely when (5.11) holds. In the limits $p \downarrow 2$ and $p \to \infty$, (5.12) simplifies to,

$$p \downarrow 2 \quad 2\sqrt{2e}(\eta_1 - \eta_2) < \gamma_1 < -\tfrac{1}{4}\sqrt{2e}\,(\eta_1 + \eta_2),$$

$$p \to \infty \quad \eta_1 - \eta_2 < \gamma_1 < -\tfrac{1}{2}\,(\eta_1 + \eta_2).$$
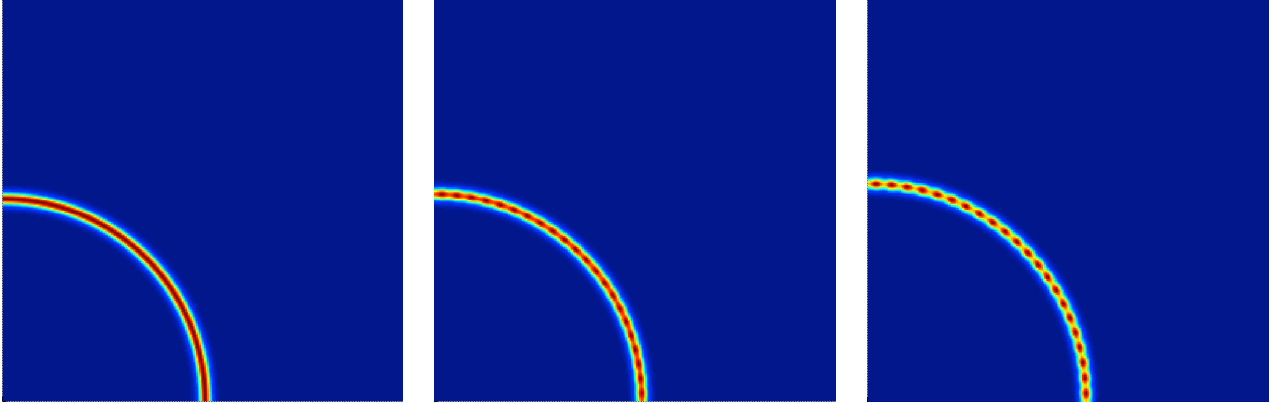
FIG. 5.1. *Images for $\varepsilon = 0.1$, $\eta_1 = \eta_2 = 2$ at times $t = 0$, $t = 114$, and $t = 804$ (left to right). A quarter of the full computational domain shown to enhance detail. The pearling is established in the second frame and converges to its equilibrium in the final frame.*
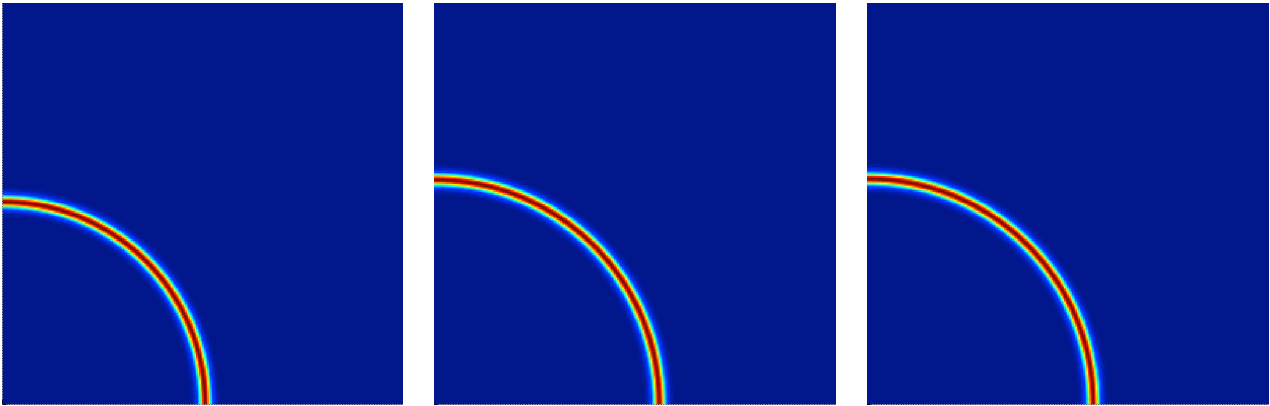

FIG. 5.2. *Images form the simulations for $\varepsilon = 0.1$, $\eta_1 = 1$, and $\eta_2 = 2$ at times $t = 0$, $t = 857$, and $t = 3000$. A quarter of the full computational domain shown to enhance detail. There is no pearling and convergence to equilibrium is substantially slower, on the $\mathcal{O}(\varepsilon^{-3})$ times scale consistent with Lemma 4.8 on the negative index of $\Pi_0 \mathbb{L}_{0,0}$, which controls relaxation of radial perturbations.*

5.2. Simulations. Numerical validation of the bifurcation conditions were performed in a doubly periodic domain $[-2\pi, 2\pi]^2$ using a general framework developed in [2], based on a Fourier spectral discretization using 512^2 modes. Fully implicit time stepping using the implicit Euler scheme was used, employing Newton's method for the nonlinear problem at each time step, and preconditioned conjugate gradient solves for each Newton step. Adaptive time stepping with a tolerance of 10^{-4} is used for each time step. The results shown below are reproduced under refinement of spatial mesh and time stepping. The potential well was taken in the form

$$W_p = \tilde{W}_p(u+1) + 20(u - \tilde{m}_p + 1)^{p+1} H(u - \tilde{m}_p + 1),$$

where H is the Heaviside function. The initial data consisted of a radial bilayer with a bilayer profile whose mass per unit length of bilayer was approximately twice the equilibrium value, suggesting that the bilayer would increase in radius, meander, or pearl to accommodate the excess mass. We took $p = 3$ for which the pearling condition (5.11) reduces to $0 < \eta_1 < \frac{2}{3}\eta_2$. We performed two runs with $\varepsilon = 0.1$ and $\mathcal{G} = -\frac{\Delta}{1-\Delta}$. Qualitatively similar results on differing time-scales were obtained for $\mathcal{G} = -\Delta$ and $G = \Pi_0$,

The first simulation, with $\eta_1 = \eta_2 = 2$, violates the pearling stability condition. The radial structure maintained its radial symmetry, however a high-frequency pearling instability was observed at time $t \approx 114$ and was subsequently maintained all the way to equilibria, see Figure 5.1. For the second simulation, with $\eta_1 = 1$ and $\eta_2 = 2$, the pearling stability condition is satisfied, and the same initial condition yielded a growing radius but did not result in pearling or meander, and converged to an equilibrium radius at $t \approx 1000$, which is consistent with an $O(\varepsilon^3)$ relaxation rate for radial perturbations, see Figure 5.2, To induce meander, we performed a third
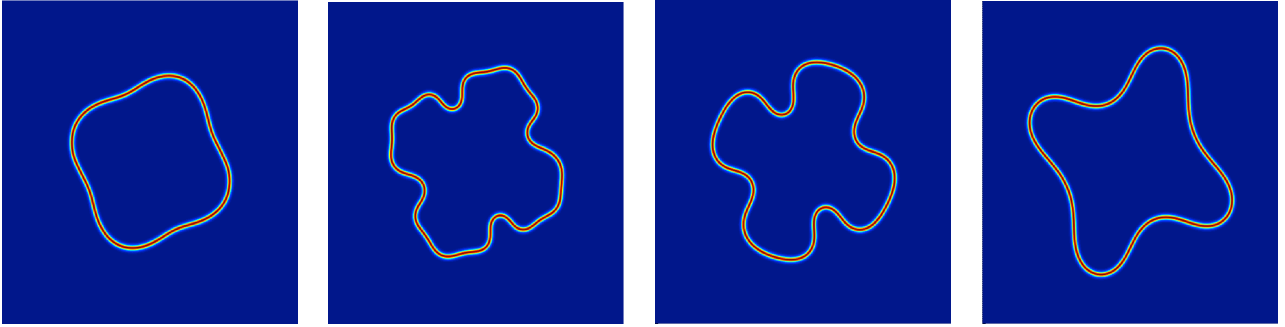
Fig. 5.3. *Images for $\varepsilon = 0.1$, $\eta_1 = 1$, and $\eta_2 = 2$ at times $t = 0$, $t = 224$, $t = 979$, and $t = 10,795$ (left to right). The initial bilayer has mass per unit length greater than M_0, and the underlying interface does not have radial symmetry. There is no pearling, however there is a strong meander which lengthens the interface, and convergence to its ultimate circular equilibrium is substantially slower, on the $\mathcal{O}(\varepsilon^{-4}) \approx 10,000$ time-scale consistent with Lemma 4.6 for the scaling of the long-wavelength meander eigenvalues which control relaxation of non-radial shape perturbations, convergence to a fully circular solution requires $t \gg 10,000$.*

simulation, with the same parameter values as the second, but non-radial initial data, given in Figure 5.3, which resulted in an initial meander transient in which the curvature of the bilayer interface increases as the interface lengthens, followed by a relaxation in which the curvature decreases and the interface converges to a radial profile on the much longer time scale associated to the $\mathcal{O}(\varepsilon^4)$ non-radial meander eigenvalues.

6. Discussion. The major results of this analysis show that the stability of bilayers is independent of the choice of admissible gradient, $\mathcal{G}$, and in the strong functionalization is independent of the curvature of the underlying interface, depending only upon the functionalization parameters and the shape of the well, W. Moreover, for $d \leq 4$ only pearling modes can drive linear instability of α-single curvature equilbria. For $d \geq 5$ meander instability is possible in the straight direction of the interface Γ if the number of curved directions, α, is greater than or equal to 3, and the radius of curvature, R_0, is sufficiently **small** or if the height, L_i, of one of the flat directions is sufficiently **large** – that is, a cylinder which is sufficiently slender, as measured by the ratio of the longest straight direction against its radius, will exhibit a meander instability in the straight direction, in space dimension greater than 4. For curved interfaces, $\alpha > 0$, the pearling instability manifests itself independent of curvature or space dimension, depending only upon the double well, W, and the functionalization parameters η_1 and η_2. However, for flat interfaces, $\alpha = 0$, the pearling instability is influenced by the background hydration level, as controlled by γ_1, with coefficient, S defined in (4.28), dependent only upon the shape of the double well. The meander eigenvalues of $\mathbb{L}$ are smaller, at $\mathcal{O}(\varepsilon^4)$, and more susceptible to perturbation, in particular the equilibrium conditions (3.18) and (3.35) play a critical role in the determination of the meander eigenvalues. For the linearization about quasi-equilbria, the meander eigenvalues generate a curvature driven flow, see [6], which can enlarge the surface area of the interface and are associated with unstable eigenvalues in the linearized flow.

REFERENCES

[1] I. Chavel [1984], *Eigenvalues in Riemannian Geometry*, Academic Press.
[2] A. Christlieb, J. Jones, K. Promislow, B. Wetton, M. Willoughby, High accuracy solutions to energy gradient flows from material science models, *J. Comp. Physics* **257** (2014) 193-215.
[3] S. Dai and K. Promislow [2013], Geometric evolution of bilayers under the functionalized Cahn-Hilliard equation, *Proc. Roy. Soc. London, Series A*, **469** no. 2153 20120505.
[4] S. Dai and K. Promislow, *Competitive geometric evolution of amphiphilic interfaces*, submitted.
[5] A. Doelman, R. A. Gardner, T.J. Kaper [2001], Large stable pulse solutions in reaction-diffusion equations, *Indiana Univ. Math. J.* **50** 443-507.
[6] N. Gavish, G. Hayrapetyan, K. Promislow, L. Yang [2011], Curvature driven flow of bi-layer interfaces, *Physica D* **240** 675-693.
[7] N. Gavish, J. Jones, Z. Xu, A. Christlieb, K. Promislow [2012], Variational Models of Network Formation and Ion Transport: Applications to Peruorosulfonate Ionomer Membranes, *Polymers* **4** 630-655.
[8] G. Gompper and M. Schick [1990], Correlation between structural and interfacial properties of amphiphilic systems, *Phys. Rev. Lett.*, **65** 1116-1119.
[9] G. Hayrapetyan and K. Promislow, *Spectra of Functionalized Operators*, to appear in *ZAMP*.
[10] P. van Heijster and B. Sandstede [2011], Planar radial spots in a three-component FitzHugh-Nagumo system, *J. Nonlinear Science* **21** 705-745.

[11] W. Hsu and T. Gierke [1983], *Ion transport and clustering in Nafion perfluorinated membranes*, Journal of Membrane Science, **13** , pp. 307-326.

[12] T. Kapitula and K. Promislow [2012], Stability indices for constrained self-adjoint operators, *Proc. American Math. Soc.* **140** 865-880.

[13] T. Kapitula and K. Promislow [2013], *Spectral and Dynamical Stability of Nonlinear Waves*, Springer, New York.

[14] N. Kraitzman and K. Promislow, *The pearling instability in curved bilayer interfaces: the strong FCH*, preprint.

[15] W. Kunz (Ed) [2009], *Specific Ion Effects*, World Scientific Publishing, New Jersey.

[16] K. Matyjaszewski [2012], Atom transfer radical polymerization (ATRP): current status and future perspectives, *Macromolecules* **45** 4015-4039.

[17] R. Mezzenga [2012], *Physics of self-assembly of lyotropic liquid crystals*, Chapter 1 of *Self-assembled supramolecular architectures*, N. Garti, P. Somasundaran, R. Mezzenga, (Eds), Wiley, N.J.

[18] P.M. Morse and H. Feshbach [1953], *Methods of Theoretical Physics*, McGraw-Hill, New York.

[19] S. Nemat-Nasser [2002], Micromechanics of actuation of ionic polymer-metal composites, *J. of Applied Physics* **92** 2899-2915.

[20] K. Promislow and H. Zhang [2013], Critical points of Functionalized Lagrangians, *Discrete and Continuous Dynamical Systems, A* **33** 1-16.

[21] M. Röger and R. Schäzle [2006], On a modified conjecture of De Giorgi, *Math. Z.* **254** 675714.

[22] N. Temme [1996], *Special Functions: An Introduction to the Classical Functions of Mathematical Physics*, John Wiley & Sons.

[23] E.C. Titchmarsh [1962], *Eigenfunction Expansions Associated with Second-order Differential Equations* (2nd ed.), Oxford Univ. Press.

[24] J. Zhu, N. Ferrer, and R. Hayward [2009], *Tuning the assembly of amphiphilic block copolymers through instabilities of solvent/water interfaces in the presence of aqueous surfactants*, Soft Matter **5** 2471-2478.

Appendix A. The proof of Lemma 5.1.

Defining $\tilde{u}_0(r) = u_0(r) + 1$, and introducing $\xi = \sqrt{\frac{2p}{p-2}}\, r$, the rescaled function $\tilde{w}_0 = \tilde{u}_0(\xi)$ is the homoclinic solution of

$$\tilde{w}_0'' - \tilde{w}_0 + \tilde{w}_0^{p-1} = 0, \tag{A.1}$$

The expressions for λ_0 and ψ_0 in (5.7) and (5.8) are determined by substitution of $\psi = (u_0 + 1)^\sigma$ into (4.19) and determining σ and λ.

Determination of M_0 and $\|\dot{u}_0\|_2^2$ (5.8). Clearly

$$M_0 = \|\tilde{u}_0\|_1 = \int_{\mathbb{R}} \tilde{u}_0(r)\, dr = \sqrt{\frac{p-2}{2p}} \int_{\mathbb{R}} \tilde{w}_0(\xi)\, d\xi. \tag{A.2}$$

Following the approach of [5], we introduce the independent variable

$$z = \frac{1}{2}\left(1 - \frac{\tilde{w}_0'}{\tilde{w}_0}\right); \tag{A.3}$$

since,

$$(\tilde{w}_0')^2 = \tilde{w}_0^2 - \frac{2}{p}\tilde{w}_0^p, \tag{A.4}$$

(A.1), it follows that

$$\tilde{w}_0^{p-2} = 2p\, z(1-z), \quad dz = (p-2)z(1-z)\, d\xi, \tag{A.5}$$

so that

$$M_0 = \frac{(2p)^{\frac{4-p}{2(p-2)}}}{\sqrt{p-2}} \int_0^1 [z(1-z)]^{\frac{3-p}{p-2}}\, dz. $$

Introducing,

$$y = 1 - 2z, \tag{A.6}$$

we find that,

$$M_0 = \left(\frac{p}{2}\right)^{\frac{4-p}{2(p-2)}} \frac{1}{\sqrt{p-2}} \int_{-1}^1 \left[1 - y^2\right]^{\frac{3-p}{p-2}}\, dy = \left(\frac{p}{2}\right)^{\frac{4-p}{2(p-2)}} \frac{2}{\sqrt{p-2}} \mathcal{I}\left(\frac{3-p}{p-2}\right) \tag{A.7}$$

which yields (5.6). The integral $\mathcal{I}(q)$ converges for $q > -1$, in particular for $q > 0$,

$$\int_0^1 (1 - y^2)^q \, dy = 2q \int_0^1 y^2 (1 - y^2)^{q-1} \, dy = 2q \left(\mathcal{I}(q-1) - \mathcal{I}(q) \right),$$

from which we deduce

$$\mathcal{I}(q) = \frac{2q}{2q+1} \mathcal{I}(q-1), \tag{A.8}$$

and (5.9) follows from (5.2) and (A.7). To determine $\|\dot{u}_0\|_2^2$, we note from (A.1) that,

$$\|\dot{u}_0\|_2^2 = \int_{\mathbb{R}} \dot{u}_0^2 \, dr = \sqrt{\frac{2p}{p-2}} \int_{\mathbb{R}} (\tilde{w}_0')^2 \, d\xi = \sqrt{\frac{2p}{p-2}} \|\tilde{w}_0'\|_2^2. \tag{A.9}$$

However from (A.4) and (A.1) we deduce that

$$\begin{array}{rcl}
\int_{\mathbb{R}} (\tilde{w}_0')^2 \, d\xi & = & \|\tilde{w}_0\|_2^2 - \frac{2}{p} \int_{\mathbb{R}} \tilde{w}_0^p \, d\xi, \\
\int_{\mathbb{R}} (\tilde{w}_0')^2 \, d\xi & = & -\int_{\mathbb{R}} \tilde{w}_0 \tilde{w}_0'' \, d\xi = -\|\tilde{w}_0\|_2^2 + \int_{\mathbb{R}} \tilde{w}_0^p \, d\xi
\end{array}$$

which yields the equalities

$$\int_{\mathbb{R}} \tilde{w}_0^p \, d\xi = \frac{2p}{p+2} \|\tilde{w}_0\|_2^2, \tag{A.10}$$

$$\|\tilde{w}_0'\|_2^2 = \frac{p-2}{p+2} \|\tilde{w}_0\|_2^2. \tag{A.11}$$

By the same procedure – i.e. by (A.3), (A.5), (A.6), (5.2), (A.8) – it follows that,

$$\|\tilde{w}_0\|_2^2 = \frac{p+2}{p-2} \tilde{m}_p^2 \, \mathcal{I}\left(\frac{2}{p-2} \right), \tag{A.12}$$

and we deduce (5.8) from (A.9) and (A.11).

The expression for S. The inhomogeneous problem $\mathcal{L}\phi_1 = 1$ (4.29) is equivalent to $\tilde{\mathcal{L}}\varphi = \frac{p-2}{2p}$, therefore we define,

$$\tilde{\varphi}_1 = \frac{2p}{p-2} \, \phi_1 \quad \text{with} \quad \tilde{\mathcal{L}}\tilde{\varphi}_1 = 1, \tag{A.13}$$

where we have introduced the scaled operator

$$\tilde{\mathcal{L}} := \frac{d^2}{d\xi^2} - \left(1 - (p-1)\tilde{w}_0^{p-2} \right), \tag{A.14}$$

The function $\tilde{\varphi}$ is even and bounded. Thus, by (5.1), (A.1), and (A.13),

$$\int_{\mathbb{R}} \phi_1 W'''(u_0) \psi_0^2 \, dr = (p-1) \sqrt{\frac{(p-2)^3}{2p}} \int_{\mathbb{R}} \tilde{\varphi}_1 \tilde{w}_0^{2p-3} \, d\xi. \tag{A.15}$$

To determine $\tilde{\varphi}_1$, we first introduce the odd function $\tilde{\Phi}_1$ and the even function $\tilde{\Phi}_2$ as the independent solutions of the homogeneous equation $\tilde{\mathcal{L}}\tilde{\Phi} = 0$. Clearly,

$$\tilde{\Phi}_1 = \tilde{w}_0', \tag{A.16}$$

where we fix $\xi = 0$ by $\tilde{w}_0'(0) = 0$ so that $\tilde{\Phi}_1$ is indeed odd; $\tilde{\Phi}_2$ can be written as

$$\tilde{\Phi}_2 = C(\xi)\tilde{w}_0'. \tag{A.17}$$

Note that $\tilde{\Phi}_2(0) \neq 0$ in general, which implies that C cannot expected to be smooth in 0. It follows that $C(\xi)$ must solve,

$$C'' \tilde{w}_0' + 2C' \tilde{w}_0'' = 0,$$

so that we can choose C' even,

$$C' = \frac{1}{(\tilde{w}_0')^2}. \tag{A.18}$$

To determine the odd solution C of (A.18) uniquely, we consider the behavior of the right hand side of (A.18) near $\xi = 0$. It follows from (5.2), (A.1), and (A.4) that,

$$\tilde{w}_0(0) = \tilde{m}_p, \quad \tilde{w}_0''(0) = -\frac{1}{2}(p-2)\tilde{m}_p,$$

so that for $|\xi|$ small enough,

$$\tilde{w}_0(\xi) = \tilde{m}_p - \frac{1}{4}(p-2)\,\tilde{m}_p\,\xi^2 + \mathcal{O}(\xi^4), \quad \tilde{w}_0'(\xi) = -\frac{1}{2}(p-2)\,\tilde{m}_p\,\xi + \mathcal{O}(\xi^3). \tag{A.19}$$

Odd function C is now determined uniquely by (A.18) and its behavior near $\xi = 0$,

$$C(\xi) = -\frac{4}{(p-2)^2\,\tilde{m}_p^2}\frac{1}{\xi}\left(1 + \mathcal{O}(\xi^2)\right), \tag{A.20}$$

for $|\xi|$ small enough. The bounded, even solution $\tilde{\varphi}_1$ (A.13) can thus be written as

$$\tilde{\varphi}_1 = A(\xi)\tilde{\Phi}_1 + B(\xi)\tilde{\Phi}_2. \tag{A.21}$$

By (A.16), (A.17), (A.19), and (A.20), the Wronskian,

$$\tilde{\Phi}_1\tilde{\Phi}_2' - \tilde{\Phi}_1'\tilde{\Phi}_2 \equiv \tilde{\Phi}_1(0)\tilde{\Phi}_2'(0) - \tilde{\Phi}_1'(0)\tilde{\Phi}_2(0) = 1,$$

hence it follows by the variation of constant approach that $A(\xi)$ and $B(\xi)$ are determined uniquely,

$$A(\xi) = -\int_0^\xi \tilde{\Phi}_2(\eta)\,d\eta, \quad B(\xi) = \tilde{w}_0. \tag{A.22}$$

From (A.13), (A.14), (A.17), (A.19), (A.20), (A.21), and (A.22) we deduce that

$$\tilde{\varphi}_1(0) = \frac{2}{p-2}, \quad \lim_{\xi\to\pm\infty}\tilde{\varphi}_1(\xi) = -1, \tag{A.23}$$

which implies that $\tilde{\varphi}(\xi)$ changes sign and thus that the sign of S is a priori not clear, see (A.15) – however, we will find that it is negative for all $p > 2$. Using (A.21) and (A.22) we write,

$$\int_{\mathbb{R}} \tilde{\varphi}_1\tilde{w}_0^{2p-3}\,d\xi = 2\int_0^\infty \tilde{\Phi}_2\,\tilde{w}_0^{2p-2}\,d\xi - 2\int_0^\infty\left(\int_0^\xi \tilde{\Phi}_2 d\eta\right)\tilde{w}_0^{2p-3}\,\tilde{w}_0'\,d\xi$$

(cf. (A.15)), so that by,

$$\int_0^\infty\left(\int_0^\xi \tilde{\Phi}_2 d\eta\right)\tilde{w}_0^{2p-3}\,\tilde{w}_0'\,d\xi = -\frac{1}{2(p-1)}\int_0^\infty \tilde{\Phi}_2\,\tilde{w}_0^{2p-2}\,d\xi,$$

it follows that,

$$\int_{\mathbb{R}}\tilde{\varphi}_1\tilde{w}_0^{2p-3}\,d\xi = \frac{2p-1}{p-1}\int_0^\infty \tilde{\Phi}_2\,\tilde{w}_0^{2p-2}\,d\xi. \tag{A.24}$$

This integral can be evaluated by one further round of integration by parts using (A.17). However, this introduces the non-smooth function $C(\xi)$ (A.20), we thus need to be more careful near 0,

$$\begin{aligned}
\int_0^\infty \tilde{\Phi}_2\,\tilde{w}_0^{2p-2}\,d\xi &= \lim_{\delta\downarrow 0}\int_\delta^\infty \tilde{\Phi}_2\,\tilde{w}_0^{2p-2}\,d\xi, = \lim_{\delta\downarrow 0}\int_\delta^\infty C\,\tilde{w}_0^{2p-2}\tilde{w}_0'\,d\xi \\
&= \frac{1}{2p-1}\lim_{\delta\downarrow 0}\left(\left[C\tilde{w}_0^{2p-1}\right]_\delta^\infty - \int_\delta^\infty C'\,\tilde{w}_0^{2p-1}\,d\xi\right), \\
&= \frac{1}{2p-1}\lim_{\delta\downarrow 0}\left(-C(\delta)\tilde{w}_0^{2p-1}(\delta) - \int_\delta^\infty \frac{\tilde{w}_0^{2p-1}}{(\tilde{w}_0')^2}\,d\xi\right), \\
&= \frac{1}{2p-1}\lim_{\delta\downarrow 0}\left(\frac{4}{(p-2)^2}\,\tilde{m}_p^{2p-3}\frac{1}{\delta} - \int_\delta^\infty \frac{\tilde{w}_0^{2p-1}}{(\tilde{w}_0')^2}\,d\xi\right).
\end{aligned} \tag{A.25}$$

However, by the transformations (A.3), (A.6), and the associated identities we find,

$$
\begin{aligned}
\int_\delta^\infty \frac{\tilde{w}_0^{2p-1}}{(\tilde{w}_0')^2}\,d\xi &= \frac{2}{p-2}\tilde{m}_p^{2p-3}\int_{\frac{1}{2}(p-2)\delta}^1 \frac{(1-y^2)^{\frac{p-1}{p-2}}}{y^2}\,dy \\
&= \frac{4}{(p-2)^2}\tilde{m}_p^{2p-3}\frac{1}{\delta} + \frac{4(p-1)}{(p-2)^2}\tilde{m}_p^{2p-3}\int_{\frac{1}{2}(p-2)\delta}^1 (1-y^2)^{\frac{1}{p-2}}\,dy.
\end{aligned}
\tag{A.26}
$$

Combining (A.25) and (A.26) yields,

$$
\int_0^\infty \tilde{\Phi}_2\,\tilde{w}_0^{2p-2}\,d\xi = -\frac{4(p-1)}{(2p-1)(p-2)^2}\tilde{m}_p^{2p-3}\,\mathcal{I}\left(\frac{1}{p-2}\right),
$$

so that (5.10) follows from (5.2), (A.15), and (A.24).